Cell Reports

Article

Wound-induced small-peptide-mediated signaling cascade, regulated by OsPSKR, dictates balance between growth and defense in rice

Graphical abstract

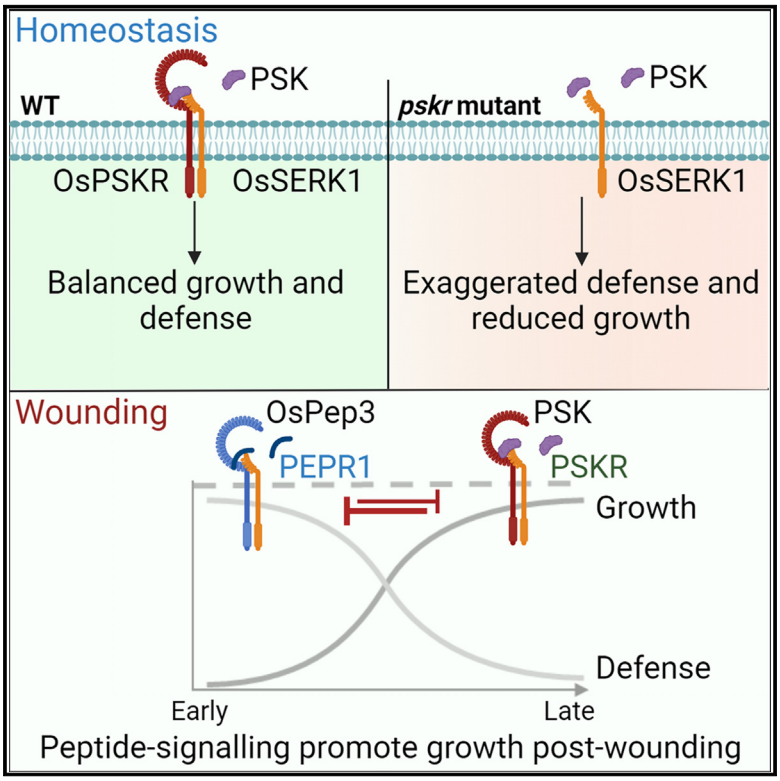

Highlights

- Wounding in rice triggers a signal relay between the small peptides OsPep3 and PSK
- OsPSKR receptor perceives PSK and plays a key role in rice growth and development
- OsPSKR dictates gene expression and promotes transition of wound responses
- OsPSKR counters OsPEPR1-mediated signaling leading to balanced growth and defense

Authors

Chitthavalli Y. Harshith, Avik Pal, Monoswi Chakraborty, Ashwin Nair, Steffi Raju, Padubidri V. Shivaprasad

Correspondence

shivaprasad@ncbs.res.in

In brief

Harshith et al. show that rice wound responses involve small-peptide-mediated signal relay between defense signaling PEPs and growth signaling by a PSK peptide hormone. OsPSKR receptor perceives PSK and maintains balance between growth and defense signaling during homeostasis and promotes growth post-wounding.

Harshith et al., 2024, Cell Reports *43*, 114515
July 23, 2024
https://doi.org/10.1016/j.celrep.2024.114515

CellPress

Cell Reports

CellPress
OPEN ACCESS

Article

Wound-induced small-peptide-mediated signaling cascade, regulated by OsPSKR, dictates balance between growth and defense in rice

Chitthavalli Y. Harshith,[1] Avik Pal,[1] Monoswi Chakraborty,[3,5] Ashwin Nair,[1,4] Steffi Raju,[1,2] and Padubidri V. Shivaprasad[1,6,*]

[1]National Centre for Biological Sciences, Tata Institute of Fundamental Research, GKVK Campus, Bellary Road, Bangalore 560065, India
[2]SASTRA University, Thirumalaisamudram, Thanjavur 613401, India
[3]Institute of Bioinformatics and Applied Biotechnology, Bangalore 560100, India
[4]Present address: HIV and AIDS Malignancy Branch, Center for Cancer Research, National Cancer Institute, Bethesda, MD, USA
[5]Present address: Department of Microbiology and Cell Biology, Montana State University, Bozeman, MT, USA
[6]Lead contact
*Correspondence: shivaprasad@ncbs.res.in
https://doi.org/10.1016/j.celrep.2024.114515

SUMMARY

Wounding is a general stress in plants that results from various pest and pathogenic infections in addition to environment-induced mechanical damages. Plants have sophisticated molecular mechanisms to recognize and respond to wounding, with those of monocots being distinct from dicots. Here, we show the involvement of two distinct categories of temporally separated, endogenously derived peptides, namely, plant elicitor peptides (PEPs) and phytosulfokine (PSK), mediating wound responses in rice. These peptides trigger a dynamic signal relay in which a receptor kinase involved in PSK perception named OsPSKR plays a major role. Perturbation of OsPSKR expression in rice leads to compromised development and constitutive autoimmune phenotypes. OsPSKR regulates the transitioning of defense to growth signals upon wounding. OsPSKR displays mutual antagonism with the OsPEPR1 receptor involved in PEP perception. Collectively, our work indicates the presence of a stepwise peptide-mediated signal relay that regulates the transition from defense to growth upon wounding in monocots.

INTRODUCTION

Plants encounter various pests, pathogens, and mechanical damages in their natural ecosystems. These encounters result in the loss of cell wall integrity (CWI). Cell wall damages are constantly monitored by various CWI sensors, and any deviation leads to various molecular and metabolic responses.[1] Persistent or unattended wound sites serve as entry points for various secondary infections and can affect the fitness of plants. The earliest molecular signaling activated by wounding is part of general stress responses that are very similar to pathogen-derived pattern triggered immune (PTI) responses. In the event of wounding, plants activate multitudes of molecular responses to initiate defense signaling that includes release of damage-associated molecular patterns (DAMPs) from the damaged cells, activation of Ca^{2+}-based signaling cascade, accumulation of reactive oxygen species (ROS) in adjacent cells, and activation of systemic signaling mediated by various phytohormones.[2,3] These responses eventually culminate in active blockage of wound site and promotion of further growth/regeneration.[4] Although most of the early wound responses are similar between monocots and dicots, monocot wound responses are not understood in detail.

Dicots have remarkable regeneration abilities, including *de novo* organogenesis.[5–7] Wounding triggers *de novo* root formation in *Arabidopsis* by the coordinated action of jasmonic acid (JA) and auxin phytohormones.[5] Auxin-mediated signaling also activates vascular regeneration post-wounding in *Arabidopsis*.[8] However, monocots lack wound-induced regeneration ability, and the wound repair process is distinct in comparison to that of dicots.[6] Upon injury, monocot leaf blades tend to display minimal cell death and initiate growth, probably owing to cell wall remodeling and cell elongation. However, the molecular mechanism involved in wound responses among monocots that have been subjected to herbivory over the course of evolution is not well understood.

Major wounding events are a direct result of insect herbivory, and the responses largely overlap between wounding and herbivory.[9] Signals emanating from endogenous sources play a major role in the activation of various signaling pathways across organisms. Plants code for a plethora of non-functional precursor proteins that code for bioactive peptides, which are further capable of activating receptor-mediated signaling pathways.[10,11] Molecular patterns derived from endogenous sources are referred to as DAMPs, and these patterns activate their cognate receptors, eventually inducing innate immunity.[12] Since

the effects of mechanical wounding and insect herbivory have been studied together, many DAMPs have been identified as major immune triggers for both responses.[13,14] Among these, systemin, an 18-amino acid (aa)-long peptide hormone specific to the *Solanaceae* family, was the first identified DAMP in response to wounding.[14,15] Other DAMPs include plant elicitor peptides (PEPs) that are well conserved across plant species and have been shown to be activated upon several cues, including wounding.[13,16–21]

PEPs are 23 aa long with varying sequences across different families.[19,22] The transcriptional dynamics that lead to the activation of downstream responses post-PEP perception are not well understood, apart from a study in which transcriptome analysis using multiple immune triggering peptides, including AtPep1, was carried out.[23] Each PEP is unique, having a distinct localization pattern, indicating the presence of species- and context-specific signaling.

Multiple studies have suggested the involvement of signal transitioning mediated by phytohormones such as JA and auxin during wounding.[5] Peptide hormones play a key role in growth and development,[24] but their specific contributions to wound responses are less well understood. Among the peptide hormones, phytosulfokine (PSK) is a sulfated pentapeptide derived from secreted precursors attributed in a multitude of roles, including cell proliferation, tracheary element differentiation, vegetative growth, lateral root development, and cell expansion.[25–28] PSK seems to be responding to wounding in *Arabidopsis*, as PSK precursors were induced upon wounding.[27,29] Whether PSK signaling actively regulates downstream wound responses is unknown. PSK is recognized by leucine-rich repeat receptor-like kinases (LRR-RLKs) across plants, and direct evidence of the binding has been provided in *Arabidopsis*, carrot, and tomato.[30–33] Although there are 15 predicted potential PSK receptors (PSKRs) in rice,[34] the nature of the signals that they respond to or their downstream functions are largely unknown. Among these, OsPSKR1 has been attributed to disease resistance,[35] while OsPSKR15 played a role in drought response.[36]

In this study, we elucidated the role of two distinct categories of small peptides in wound perception and response in rice using time course transcriptome analysis. We identified an early activation of *OsPROPEP3* upon wounding, which is the precursor for OsPep3. Furthermore, wound-triggered PEP signaling activated a peptide hormone, PSK. Using *in silico*, *in vitro*, and *in vivo* methods, we identified OsPSKR as a receptor for PSK. We found that OsPSKR plays an essential role in development since its mutants displayed drastic phenotypes, including sterility. We also identified its role in maintaining balance between growth and defense responses under homeostasis. During wound responses, OsPSKR assisted in transitioning from early defense responses to late growth/repair responses by suppressing late wound-responsive genes. We have also found a clear antagonistic crosstalk between growth signaling OsPSKR and defense signaling OsPEPR1-derived processes. These findings suggest the presence of a stepwise transcriptional program that relays wound-induced signals through a receptor-kinase that dictates growth vs. defense responses in rice.

RESULTS

Time course transcriptome screen identifies rapid induction of precursors of small peptides upon wounding

Among dicots, the earliest transcriptional responses to wounding include rapid expression of peptide precursors and various wound-responsive genes.[2,3] Since a detailed understanding of temporal progression of specific events among monocots upon wounding is lacking,[6,7] a detailed multi-time point transcriptome analysis was carried out using 6-week-old rice seedlings. Wounding was carried out by punching leaf blades,[37] and samples were collected at 15 min, 30 min, 2 h, and 12 h post-wounding with appropriate unwounded controls (Figure 1A). RNA sequencing (RNA-seq) datasets were generated in biological duplicates and processed as described.[38] The number of differentially expressed genes (DEGs) increased over the time after wounding, indicating a gradually intensifying response (Figure 1B; Table S3). Studies in *Arabidopsis* have identified JA-related genes as one of the earliest responding sets of genes to wounding.[5] Similarly, wounding in rice also triggered JA signaling-related genes at early time points (15 and 30 min), in addition to other genes involved in signaling (Figure S1A). JA pathway genes *OsJAZ11* and *OsAOS1* showed a rapid response to wounding, with increasing expression over time (Figure 1C). However, in contrast to JA pathway genes, salicylic acid (SA) biosynthesis gene *OsICS1* did not respond to wounding as these two phytohormone pathways are antagonistic to each other.[39] Two of the well-studied general stress-responsive WRKY transcription factors, *OsWRKY45* and *OsWRKY53*, also showed transcriptional upregulation upon wounding (Figure 1C).

Many studies have shown the induction of small-peptide coding genes either upon mechanical wounding or upon insect herbivory.[2] We explored the transcriptional response of precursors of small-peptide coding genes and their homologs.[11] These included a total of 54 small-peptide coding precursors, including PSKs, RALFs, PROPEPs, and PSYs.[16,28,40,41] Among these precursors, two different peptide precursors belonging to distinct categories were found responding to wounding (Figure 1D; Table S3). *OsPROPEP3*, a gene that codes for a DAMP called OsPep3 showed a remarkable induction at a very early time point post-wounding. *OsPROPEP3* was previously identified to be wound responsive as well as responsive to herbivore-derived oral secretion in rice.[16] Rapid upregulation of *OsPROPEP3* and subsequent reduction beyond 30 min post-wounding was confirmed using qRT-PCR (Figure 1E). Rice has a total of six predicted PROPEPs with varying sequences and gave rise to bioactive peptides of 23 aa in length (Figure S1B).

To understand whether bioactive peptide derived from OsPROPEP3 can elicit wound responses, rice leaves were treated with OsPep3 peptide and OsPep2, previously attributed to herbivore responses.[18] MPK activation is one of the primary hallmarks of PTI activation, and many studies have shown that PEPs can activate MPK signaling.[16,42] In agreement with this, we observed a rapid activation of MPK post-wounding, as well as upon OsPep3 and OsPep2 treatments,

CellPress
OPEN ACCESS

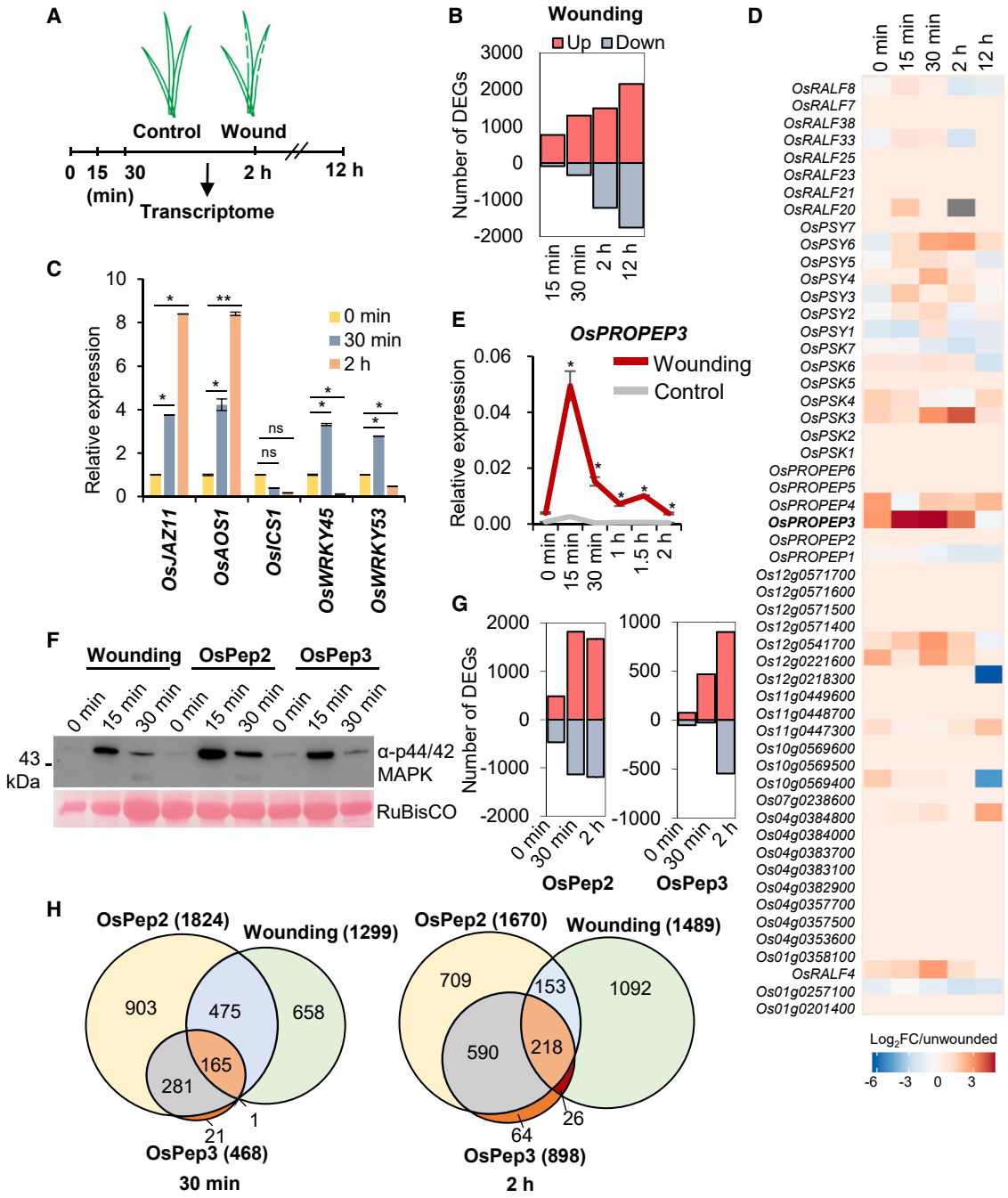

Figure 1. Time course transcriptome screen identifies rapid induction of precursors of small peptides upon wounding

(A) Scheme showing the wounding experiment and sample collection time points.

(B) Differential expression of genes upon wounding across time points.

(C) qRT-PCR analysis of expression of *OsJAZ11*, *OsAOS1*, *OsICS1*, *OsWRKY45*, and *OsWRKY53* relative to *OsActin* upon wounding.

(D) Transcriptional changes of precursors of various DAMPs represented as $\log_2$ fold change (FC) with respect to corresponding unwounded samples.

(E) RT-qPCR analysis of expression of *OsPROPEP3* relative to *OsActin* upon wounding.

(F) MPK activation assay upon wounding, OsPep2 and OsPep3 treatments. Leaf strips were treated with 1 μM of peptides.

(G) Number of significantly differentially regulated genes upon OsPep2 and OsPep3 treatments.

(H) Representation of the number of overlapping upregulated genes between wounding, OsPep2, and OsPep3 treatments. Upregulated, $\log_2FC \geq 1.5$; downregulated, $\log_2FC \leq -1.5$, $p < 0.05$.

$n = 3$ for all qPCR experiments, error bars indicate standard error of the mean (SEM), pairwise Student's t test with respect to 0-min samples; $^*p < 0.05$; $^{**}p < 0.005$.

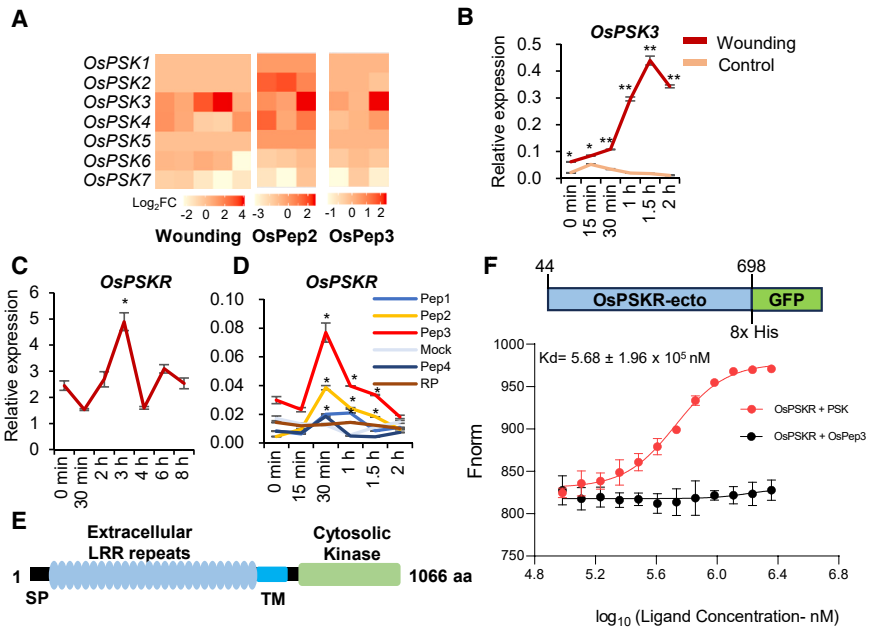

Figure 2. Wounding and wound-derived OsPep3 treatments activated PSK signaling

(A) Expression profile of predicted OsPSK precursors upon wounding, OsPep2, and OsPep3 treatment.

(B) qRT-PCR showing the transcriptional upregulation of *OsPSK3* relative to *OsActin* upon wounding, $n = 3$.

(C) qRT-PCR analysis of expression of *OsPSKR* relative to *OsActin* upon wounding across time points, $n = 9$.

(D) qRT-PCR analysis of expression of *OsPSKR* relative to *OsActin* upon peptide treatment across time points, $n = 3$.

(E) Domain architecture of OsPSKR. SP, signal peptide; TM, transmembrane.

(F) MST assay showing the binding of PSK to OsPSKR represented as normalized fluorescence values. Ligand concentration is presented as $\log_{10}$ values. Kd value was estimated using analysis software provided by the manufacturer. Kd, dissociation constant.

For all qRT-PCR experiments, error bars in all the graphs indicate SEM, pairwise Student's t test with respect to control samples; $^{*}p < 0.05$, $^{**}p < 0.005$.

suggesting the activation of conventional PTI signaling (Figure 1F). We also confirmed transcript upregulation of OsMPK3 upon wounding, as well as OsPep3 and OsPep2 treatments (Figures S1C and S1D). To identify the molecular responses activated by OsPep3 and OsPep2, and to assess the similarities and overlap between the responses activated by wounding and PEP treatment, we performed a transcriptome analysis after treating rice leaves using OsPep3 and OsPep2. Both OsPep3 and OsPep2 treatments led to differential expression of several hundred genes (Figure 1G; Table S3).

To further understand whether the genes responsive to OsPep3 and OsPep2 treatments are under wound-response module, we overlapped genes responding to individual treatments with one another (Figure 1H). We noticed that over 90% of the genes responsive to OsPep3 were also responsive to OsPep2, indicating the remarkable similarities between downstream responses upon PEP perception. Also, we observed a strong overlap of 49.2% (30 min) and 24.91% (2 h) between PEP-responsive (upregulated) and wound-responsive (upregulated) genes across two different time points, indicating that PEPs can trigger responses similar to wounding. The categories of genes responding to wounding changed over time, with the early set of genes predominantly involved in JA signaling and the late set of genes involved in ribosome subunit biogenesis and rRNA processing (Figure S1A). Both OsPep3 and OsPep2 treatments triggered a similar set of genes that were upregulated 30 min post-wounding (Figure S1E). These results suggest that mechanical wounding induced a rapid transcriptional signaling, including the induction of peptide-coding genes. Bioactive peptides that are derivatives of precursor genes induced similar responses to that of wounding, indicating a surprising functional resemblance of downstream signaling.

Wounding and wound-derived OsPep3 treatments activated PSK signaling

Previous studies have shown that transcriptional dynamics upon wounding involved transitioning from early defense responses to late growth responses.[4,5] To explore this possibility, we compared transcriptomes between early vs. late time points. We observed a delayed upregulation of a precursor of a distinct category of small peptides, PSK (Figure 2A; Table S4). There are seven predicted PSK coding genes in rice, and among these, *OsPSK3* showed a remarkable induction at 2 h post-wounding. This response was also observed with OsPep2 and OsPep3 treatments, indicating that PSK activation at a delayed time point might be under the regulation of a signal relay (Figure 2A). qRT-PCR analysis of the expression dynamics of *OsPSK3* upon wounding showed an induction 1 h post-wounding, indicating a possible peptide-mediated temporal signaling relay either hierarchically or parallel, since *OsPROPEP3* induction was observed at 15 min post-wounding (Figures 1D and 2B). Induction of PSK upon wounding was also observed in *Arabidopsis*, but at a much later time point,[27,29] where it was perceived by an LRR-RLK called AtPSKR1.[30] The exact role and mechanism of PSK signaling in wound responses has not been explored. Induction of *OsPSK3* upon wounding as well as with OsPep3 treatment indicates the specific activation of PSK-mediated signaling.

To ascertain the probable role of a PSK receptor in the transduction of signals upon wounding, we considered all 15 rice PSK receptors predicted previously.[34,35] Transcriptome analysis showed differential regulation of several predicted PSK receptor genes upon wounding as well as with OsPep3 treatment (Figure S2A; Table S4). However, since PSK upregulation was observed around 2 h post-wounding, we reasoned that receptor genes might be transcriptionally upregulated after 2 h. qRT-PCR analysis indicated that *OsPSKR4*, *-7*, and *-8* showed a very early induction (Figure S2B). Although these might contribute in part to

wound response, they were unlikely to be involved in wound-induced PSK perception, which is triggered in a delayed manner. *OsPSKR5*, *6*, and *10* did not show induction post-wounding (Figure S2B). However, we observed a clear and pronounced induction of *OsPSKR*, also known as *OsPSKR12*, which exhibited sharp upregulation 3 h post-wounding (Figure 2C). Interestingly, *OsPSKR* was highly upregulated upon OsPep3 treatment, and to a lesser extent upon OsPep2 treatment and not with other peptides tested (Figures 2D and S2A). OsPSKR is a close homolog of AtPSKR1 and DcPSKR, and was previously implicated in insect herbivory responses called OsLRR-RLK1.[43] OsPSKR possesses extracellular leucine-rich repeats, a single-pass transmembrane region, and a cytosolic kinase domain (Figure 2E). Phylogenetic analysis using well-studied ligand binding receptors in *Arabidopsis* and rice, along with all 15 predicted potential PSK receptors, indicated that OsPSKR was closely related to PSK receptors in *Arabidopsis*, indicating a possibility that OsPSKR might be involved in the perception of PSK (Figure S2C). A homology-based model of the protein using the AtPSKR1 structure as a reference[30] was generated to explore whether PSK directly interacted with OsPSKR. Docking experiments revealed that PSK potentially interacted with OsPSKR (Figure S2D). Molecular dynamics (MD) simulations were conducted to ascertain protein conformations in the presence of ligand. Root-mean-square deviation plots revealed slightly higher stability of the protein backbone in the presence of ligand (Figures S2E and S2F). Probable residues taking part in ligand-receptor interactions were deduced from MD simulation experiments, with K432 and N433 displaying strong interactions (Figure S2G). Docking performed using K432A and N433A mutants indicated a lack of interactions, as expected (Figure S2H). To validate this experimental, extracellular region of OsPSKR (residues 44–698) was expressed and purified in codon plus strain of *Escherichia coli*. The protein was subjected to microscale thermophoresis (MST) assay with ligand. OsPSKR showed strong binding to PSK in a dose-dependent manner, and this was absent when OsPep3 acting as negative control was used, suggesting that OsPSKR specifically bound to PSK (Figures 2F and S2I). These results suggest that wounding and wound-derived peptides activate PSK signaling that is perceived by OsPSKR. This signaling likely mediates activation of downstream responses.

OsPSKR is a catalytically active kinase that associates with co-receptor OsSERK1

Ligand recognition by LRR-RLKs leads to the activation of a pattern recognition receptor (PRR) complex that consists of a cognate receptor, a co-receptor, and a receptor-like cytoplasmic kinase.[44] OsPSKR belongs to the subfamily LRR-Xb[45] and RD group of RLKs since it has the conserved HRD motif in the catalytic domain. It has been proposed that the RD group of kinases function in a catalytic activity-dependent manner.[46,47] Since OsPSKR possesses a predicted cytosolic kinase domain (KD), we performed an *in vitro* phosphorylation assay to assess its kinase activity. We purified the KD of OsPSKR and the mutant of the KD (ΔKD) with mutations in an ATP binding site (K814E) and catalytic motif (D912N) (Figure 3A). We did not notice any autophosphorylation when KD alone was used (Figure S3A). In many RLKs, it has been shown that the residues undergoing phosphorylation are mostly present in the juxtamembrane (JM) region of the proteins.[44] Therefore, we considered KD with JM region for subsequent assays (Figure 3A). The AtEFR cytosolic domain, which was previously shown to undergo autophosphorylation,[47] as well as its kinase dead version, were also purified and used as controls in our experiment. We detected the phosphorylation signal with the cytosolic domain of OsPSKR and AtEFR, but not in the mutated versions of these proteins, suggesting that OsPSKR is a true kinase (Figure 3B). Most PRRs associate with co-receptors such as AtBAK1 upon ligand binding before activating a series of transphosphorylation events.[48] Rice has two homologs of AtBAK1, OsSERK1 and OsSERK2, with about 79% aa similarity with each other. To check the possible association of these homologs with OsPSKR, first, OsPSKR-GFP or GFP expression in *Nicotiana benthamiana* was confirmed using western blotting (WB) (Figure S3B). Co-expression of OsPSKR and OsSERK2 abolished/reduced the accumulation of both proteins, and this was independent of PSK treatment, indicating that OsSERK2 was not likely a co-receptor for OsPSKR (Figures 3C and S3C). Therefore, we considered OsSERK1 alone for further experiments. We co-infiltrated OsPSKR-GFP or its KD mutant (OsPSKRΔKD-GFP) with OsSERK1, followed by super-infiltration of PSK. WB analysis revealed that the accumulation of OsPSKR increased in the presence of PSK treatment. This PSK-induced stability of OsPSKR was not prominent in the KD mutant (Figures 3D, S3D, and S3E). PSK-induced enhanced accumulation of OsPSKR was also observed in rice plants expressing GFP-tagged OsPSKR. This accumulation was more pronounced in the presence of MG132, a proteasome inhibitor, indicating a possible proteostatic regulation (Figure 3E). These results suggest that ligand treatment stabilizes the receptor, and this is possibly dependent on the kinase activity of OsPSKR. We further explored whether OsPSKR directly interacted with OsSERK1, its likely co-receptor. We co-infiltrated OsPSKR with OsSERK1, followed by super-infiltration (infiltration with peptide solution 2 days post-infiltration) of 1 μM PSK or water as control for 20 min. These samples were subjected to immunoprecipitation (IP) of OsPSKR-GFP or GFP. WB analysis indicated the interaction between OsPSKR and OsSERK1, indicating that they are a bona fide receptor-co-receptor pair (Figures 3F and S3F). The interaction did not seem to depend on PSK treatment (Figure 3F). However, endogenous PSK from *N. benthamiana* plants might have played a role in the observed interaction in the absence of exogenous PSK application (Figure 3F). Also, it has been shown in *Arabidopsis* that PSK is not essential for PSKR-SERK interaction.[30] Nevertheless, these results clearly show that OsPSKR is a catalytically active kinase, and interaction with PSK ligand results in its stabilization, indicating that PSK is the cognate ligand of OsPSKR. Furthermore, OsSERK1 is the co-receptor for OsPSKR and interacts with OsPSKR, irrespective of exogenous PSK application.

OsPSKR knockout (KO) plants displayed major growth and reproductive defects

To understand the importance of OsPSKR in plant development, and wound response in particular, we generated CRISPR-Cas9-mediated KO plants using construct harboring guide RNA

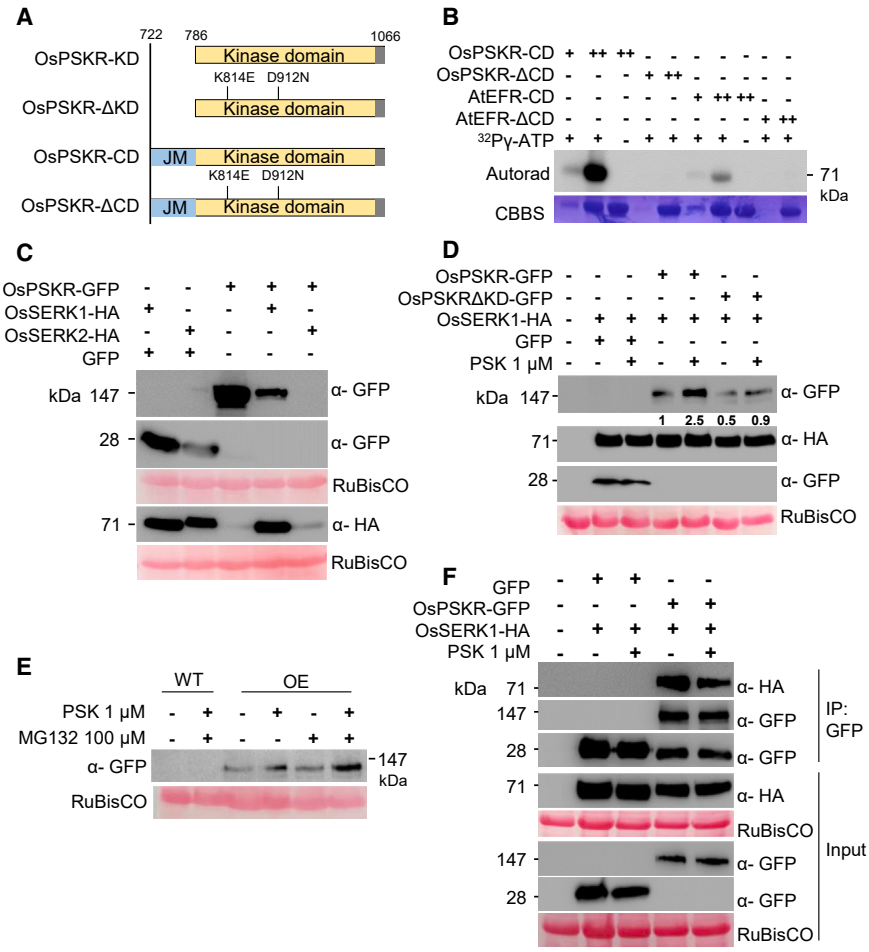

Figure 3. OsPSKR is a catalytically active kinase and associates with OsSERK1

(A) Depiction of kinase and JM region of OsPSKR used for kinase assays. CD, cytosolic domain; KD, kinase domain.

(B) OsPSKR is a functional kinase and undergoes autophosphorylation. Autorad, phosphor signal; CBBS, Coomassie brilliant blue.

(C) Immunoblots showing the accumulation of OsPSKR and OsSERK1/2 in infiltrated *N. benthamiana* plants.

(D) Immunoblots showing the co-expression of OsPSKR/OsPSKRΔKD with OsSERK1 in *N. benthamiana*.

(E) WB showing PSK-induced accumulation of OsPSKR in OsPSKR OE rice plants.

(F) IP assay showing interaction between OsPSKR and OsSERK1 in the presence or absence of PSK in *N. benthamiana*.

specific to OsPSKR (Figure S4A). We obtained three independent lines. The nature of mutations in these lines included a 2-nt deletion in KO-1 and single-nucleotide insertions in both KO-2 and KO-3 transgenic lines (Figure S4B). All these mutations led to premature stop codons, with KO-1 terminating at 141 aa and KO-2 and KO-3 terminating at 142 aa. Since these plants had very drastic phenotypes, where the plants failed to make any viable seeds, we also generated artificial microRNA (amiR)-mediated knockdown (*kd*) lines (Figure S4F). amiR that can target OsPSKR, but not other OsPSKRs, designed through the WMD3 tool,[49,50] incorporating position-specific GC signatures that improve amiRNA targeting that we deduced previously[51] was used for generating transgenic lines. The three *kd* plants obtained exhibited slow growth and reduced fertility, similar to that of KO plants (Figures 4A and 4B). The expression of amiR was confirmed using northern blotting (Figure S4G). All *kd* plants had a more than 50% reduction in transcript levels exhibiting partial sterility (Figure S4H). KO plants had reduced height, had increased tiller numbers, and were completely sterile (Figure 4A). Surprisingly, there was an increased number of tillers in KO plants, suggesting a possible compensatory effect (Figure 4D). The flowers, when developed, had unusual stigma and style and imperfectly developed palea and lemma (Figures 4E, S4D, and S4E). The pollen grains failed to form in KO plants, indicating that reproductive development was completely affected (Figures 4F and S4C). Microcomputed tomography (micro-CT) and scanning electron microscopy (SEM) images of individual florets and walls of anthers and stigma indicated hollow anthers, shrunken anther walls, and reduced stigma branching (Figures 4G–4I).

We also generated lines overexpressing (OE) OsPSKR under constitutive 35S promoter with GFP tag at the C terminus (Figure S5A). We obtained a total of eight plants with two independent transfer DNA insertion events, with four plants having single-copy insertions (Figure S5B). All plants had increased expression of the transgene (Figure S5C). Accumulation of OsPSKR-GFP transgenic protein was confirmed using confocal imaging (Figure S5D), which also indicated membrane localization, expected of PRRs. The OE plants clearly showed growth benefits (Figure 4C). The root growth and shoot growth was better in OE plants compared to wild type (WT), indicating the positive regulation of growth by OsPSKR (Figures S5E and S5F). The transcriptome profiling of OE plants showed the upregulation of various growth-associated genes, indicating that OsPSKR is a promoter of growth (Figure S5G; Table S5). Furthermore, to check whether KO plants responded to PSK treatment, we performed PSK treatment of WT and KO leaves across three different time points: 30 min, 2 h, and 4 h. Transcriptome analysis of the samples indicated that the KO plants were almost insensitive to PSK. This indicated that OsPSKR alone is specifically involved in PSK perception without the possibility of functional redundancy between other PSK receptors in PSK perception, at least for the time points tested (Figure 4J; Table S5). Gene Ontology (GO) analysis of genes upregulated upon PSK treatment showed the predominant enrichment of photosynthesis-related genes (Figures S5H and S5I). Together,

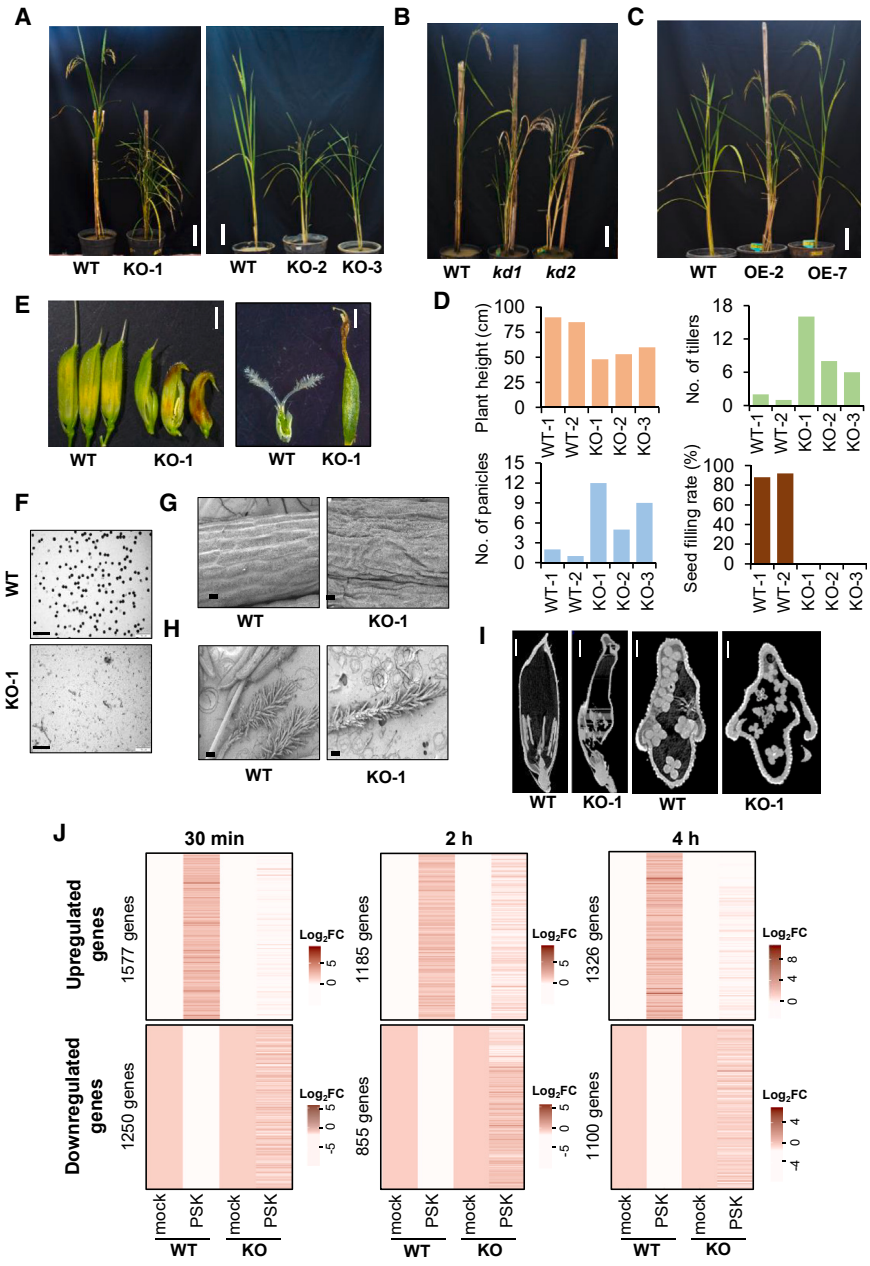

Figure 4. OsPSKR KO plants display major developmental defects and are insensitive to PSK treatment

(A) OsPSKR KO plants (12-week-old). Scale bars, 8 cm.

(B) Phenotype of OsPSKR knockdown plants. Scale bars, 8 cm.

(C) OsPSKR OE plants. Scale bar, 7 cm.

(D) Measurement of morphological defects in KO plants (plotted for individual plants).

(E) KO plants show defective grains (scale bar, 0.25 cm) and stigma (scale bar, 1 mm).

(F) Iodine staining of pollen grains in KO plants. Scale bar, 200 μm.

(G) SEM images of anther. Scale bar, 20 μm.

(H) SEM images of stigma. Scale bar, 100 μm.

(I) Micro-CT images of grains. Scale bars, 800 μm.

(J) Transcriptome profiling of WT and KO plants upon PSK treatment across time points.

these results indicated that OsPSKR, a bona fide receptor of PSK, is an essential gene in rice development, and its involvement in wound response might be crucial for rice plants in countering stresses.

OsPSKR positively regulated early wound responses

To understand the specific roles of OsPSKR in the regulation of wound responses and other developmental processes, we performed transcriptome analyses of both KO and OE lines. We identified perturbed expression of several genes in both cases (Figure S6A; Table S6). Genes upregulated in KO plants were predominantly involved in purine metabolism and photosynthesis, as shown by GO analysis. Downregulated genes in KO included those involved in various metabolic processes, including response to wounding category (Figure S6B). In the case of upregulated genes in OsPSKR OE, most were involved in responses to biotic factors and signal transduction. However, downregulated genes were involved mainly in rRNA processing (Figure S6C). We further sought to ascertain specific wound-response regulation dictated by OsPSKR. Callose deposition is one of the primary responses in case of wounding as well as PTI activation.[2] We assessed callose deposition in KO plants 1 h post-wounding by subjecting wounded samples to aniline blue staining. We observed the absence of callose deposits in KO plants, indicating that OsPSKR positively regulates wound responses and contributes to callose deposition (Figures 5A and S6D). AtPEN3 protein belonging to the ABCG transporter class has been attributed to pathogen-induced callose deposition in *Arabidopsis*.[52] The expression of rice homologs of AtPEN3 such as *OsABCG37*, *-39*, and *-45* was upregulated upon wounding in WT, but they were either not upregulated or showed reduced upregulation in KO plants (Figure 5B), suggesting direct regulation of expression of these genes by OsPSKR.

To further understand the transcriptional dynamics downstream to OsPSKR, which might be part of PSK signaling, we compared the genes that were upregulated in the case of OsPSKR OE and the genes that were downregulated in KO plants. We found 80 genes that were common for both sets, indicating that these genes were under direct regulation of signaling mediated by OsPSKR (Figure 5C). GO analysis of these 80 genes indicated their involvement in various metabolic processes, including wounding (Figure 5D). We further overlapped the

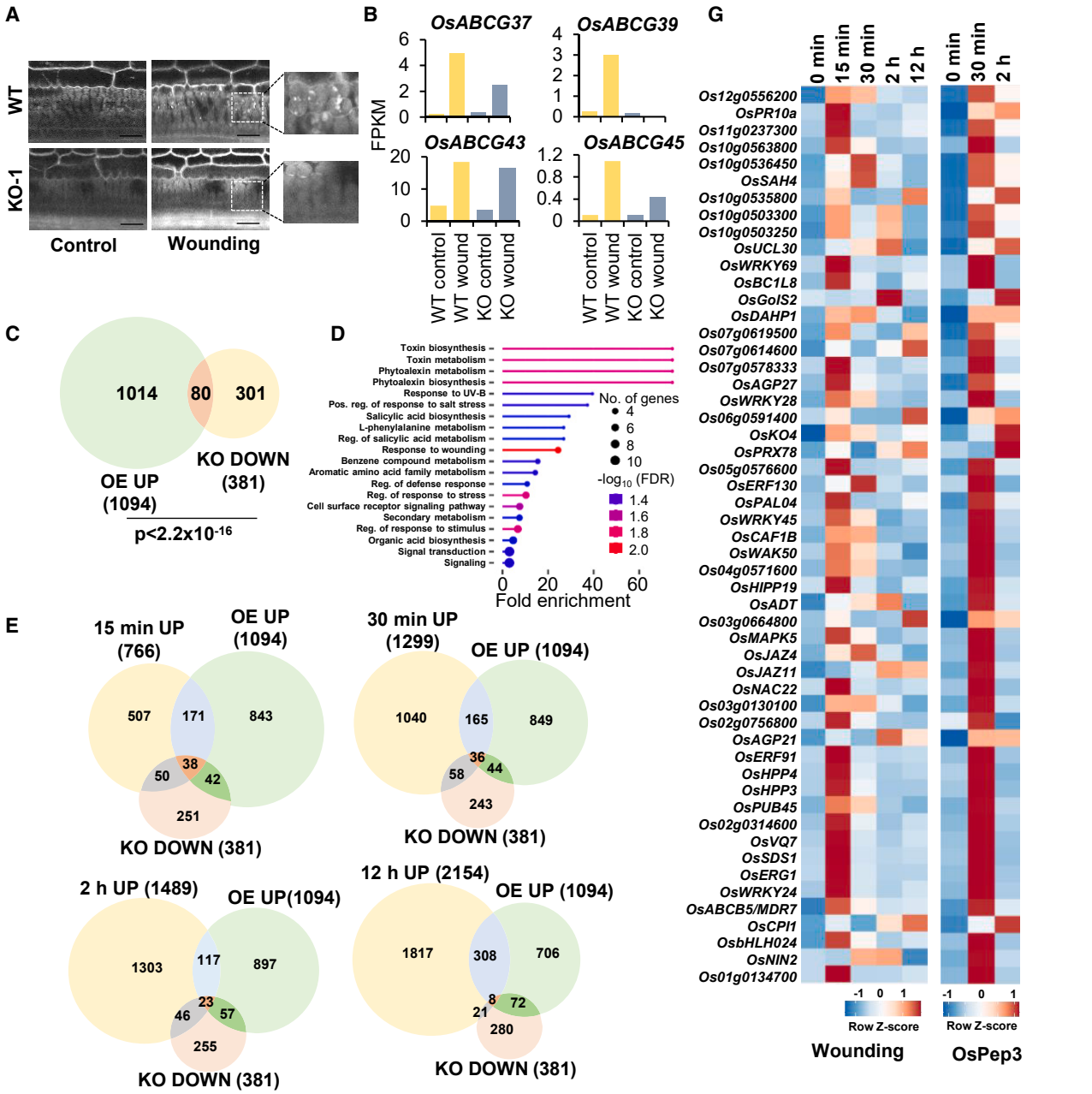

(legend on next page)

upregulated genes post-wounding across time points with genes upregulated in OsPSKR OE and downregulated in KO plants (Figure 5E). We obtained 53 genes that were unique and were common to all three sets—upregulated upon wounding across time scales, upregulated in OsPSKR OE lines, and downregulated in KO plants. These 53 genes included some of the homologs of well-studied wound-responsive genes. These include four WRKY transcription factors (*OsWRKY24*, *OsWRKY28*, *OsWRKY45* and *OsWRKY69*); an MPK (*OsMAPK5*); ERF transcription factors *OsERF91* and *OsERF130*; two JAZ repressors (*OsJAZ4* and *OsJAZ11*); a VQ domain containing genes *OsVQ7* and *OsNAC22*; a basic helix-loop-helix transcription factor, *OsCAF1B*; and many others (Figure 5G; Table S6). These results further indicate that OsPSKR is a hub that mediates wound responses in rice. In agreement with this, we observed that the expression of some of the key wound-responsive genes was positively impacted in OE and negatively impacted in KO plants upon wounding (Figure 5F). These genes included *OsAOS1* (involved in JA biosynthesis), *OsWRKY45* (a general stress-responsive WRKY transcription factor), and *OsJAZ11* (a gene involved in the repression of the JA signaling pathway).[53] However, *OsICS1*, which is not wound responsive in WT plants, showed a contrasting trend in KO plants, suggesting an antagonistic regulation of *OsICS1* by OsPSKR (Figures 1C and 5F). Interestingly, many of the wound-responsive genes that were under positive regulation of OsPSKR were also responsive to OsPep3 treatment, indicating similarities between signals activated by wounding and wound-derived PEP treatment (Figure 5G; Table S6). Together, these analyses and results suggest that OsPSKR acts as a positive regulator of early wound responses as observed in callose deposition, as well as transcriptional response of some of the early wound-responsive genes. Also, OsPep3 activated a set of genes similar to those that were under direct regulation of OsPSKR, indicating a conserved and integrated regulation of responses to wounding.

OsPSKR assists in signal transitioning by negatively regulating late wound responses

KO plants displayed a constitutive cell death phenotype. Cell death and necrosis were more evident near the leaf tips. We performed trypan blue staining and 3,3′-diaminobenzidine (DAB) staining of the leaves obtained from all three KO plants. All three plants displayed constitutive activation of cell death (Figure 6A). DAB staining revealed exaggerated accumulation of ROS in these plants (Figure 6B). These phenotypes are suggestive of the negative regulation of constitutive defense responses by OsPSKR during homeostatic conditions. To understand the regulation in detail, we subjected the cell death-displaying leaves from KO to transcriptome profiling. Strikingly, around 50% of the differentially expressed transcriptome of cell death-exhibiting leaves was identical to that of the differentially expressed transcriptome post-12 h of wounding (Figure 6C). We then performed GO analysis of the genes that were upregulated upon wounding and upregulated in the case of cell death-displaying KO plants. We observed a great similarity, and most of them were involved in rRNA modification and processing (Figure S7A). Very surprisingly, similar sets of genes were downregulated in OE plants (Figure S7A). These results clearly indicate that during homeostasis, OsPSKR keeps late wound-responsive genes under check to prevent excessive defense signaling. Therefore, we hypothesized that OsPSKR plays an important regulatory role post-wounding by assisting smoother transitioning from early to late wound responses. This necessitated the identification of the nature of DEGs responding to wound response in KO and OE after the 12-h time point.

To capture the wound responses, we considered all the differentially regulated genes in WT post-12 h. There were 2,154 and 1,751 genes that were upregulated and downregulated, respectively, in WT. Surprisingly, the same genes did not show any response to wounding in the case of OE plants. In KO, there was an exaggerated response for around 50% of the genes, indicating that OsPSKR-mediated signaling acted as a checkpoint in WT plants, as these genes were highly suppressed in OE plants (Figures 6D and 6E; Table S7). These results indicated that the presence of OsPSKR is essential for normal wound responses. Since we observed complete suppression of late wound-responsive transcriptome in the case of OE, it is possible that the increased dosage of OsPSKR led to the early transition to late wound responses. However, in KO, this transition was almost completely perturbed, as expected (Figure 6F).

Since KO plants showed cell death phenotypes, it is possible that cell death-causing genes could be highly misregulated post-wounding in KO. Some of the NAC transcription factors have been attributed to hypersensitive responses that lead to the cell death phenotype. Increased expression of *OsNAC4* was shown to activate the cell death phenotype.[54] OsNAC2 was shown to be a regulator of salt-induced cell death.[55] Our transcriptome, as well as qRT-PCR analysis, showed the upregulation of *OsNAC2* and *OsNAC4* upon wounding in WT plants. The expression of these genes in KO plants upon wounding was similar to that in WT wounded plants. *OsNAC2* was constitutively upregulated in KO plants. However, such a wound-induced upregulation of *OsNAC2* and *OsNAC4* was not observed in OE plants, indicating that OsPSKR suppresses cell

Figure 5. OsPSKR positively regulates early wound responses

(A) Images showing callose deposition at 1 h post-wounding in WT and KO leaves. Scale bars, 25 μm.

(B) Expression pattern (FPKM values) of ABCG transporters upon wounding in WT and KO plants.

(C) Venn diagram representing genes overlapping between upregulated genes in OE and downregulated genes in KO. *p* value obtained from Fisher's exact test.

(D) GO analysis of genes overlapping between OE upregulated and KO downregulated sets.

(E) Representation of overlap between wound-responsive genes and genes under OsPSKR regulation across time points.

(F) qRT-PCR analysis of *OsAOS1*, *OsWRKY45*, *OsJAZ11*, and *OsICS1* relative to *OsActin* upon wounding in WT and KO plants. $n = 3$, error bars indicate SEM, pairwise Student's t test with respect to 0-min samples. $^{**}p < 0.05$; $^{***}p < 0.005$.

(G) Transcriptional dynamics of 53 wound-responsive genes under OsPSKR regulation upon wounding and OsPep3 treatment. Row *Z* score values were calculated using FPKM values.

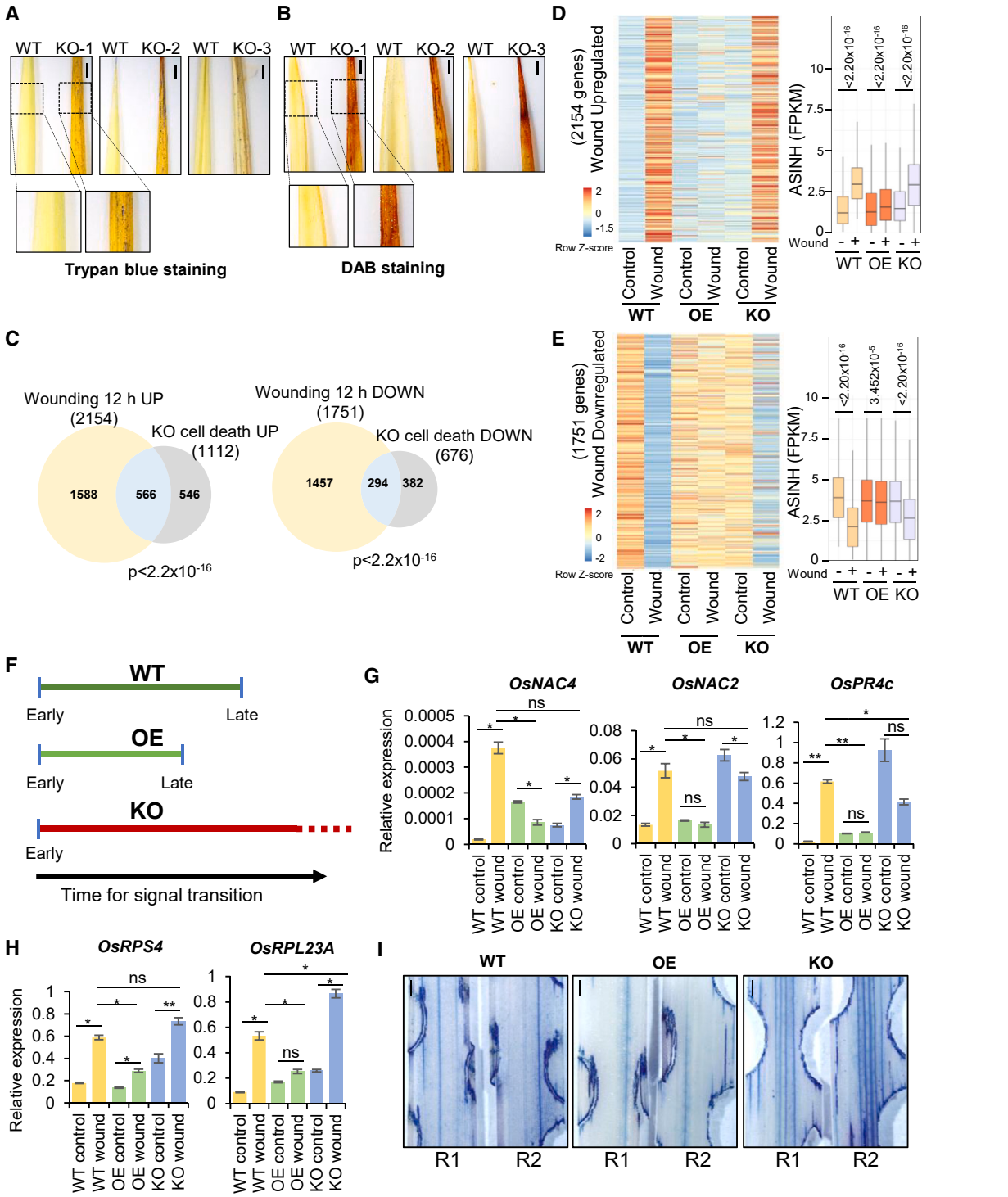

Figure 6. OsPSKR assists in signal transitioning by negatively regulating late wound responses

(A) Trypan blue staining indicates constitutive cell death phenotypes in KO plants. Scale bars, 1 mm.

(B) DAB staining for ROS accumulation in KO plants. Scale bars, 1 mm.

(C) Overlap between wound-responsive genes and DEGs in KO (cell death-showing leaves), *p* values obtained from Fisher's exact test.

(D and E) Transcriptional dynamics of wound-responsive genes in transgenics, ASINH-transformed FPKM values were plotted correspondingly; *p* values obtained from Wilcoxon test.

(legend continued on next page)

death inducers upon wounding (Figure 6G). *OsPR4c*, a pathogenesis-related gene, was upregulated in KO plants, and it was wound responsive in WT plants. Its induction was suppressed in OE plants, suggestive of defense gene suppression upon wounding by OsPSKR (Figure 6G).

In addition, we observed that ribosomal protein-coding genes were upregulated upon wounding in WT plants. Strikingly, a similar set of genes were upregulated in KO plants and were suppressed in OE plants, suggesting the role of OsPSKR in translation. Deregulated translation has been attributed to cell death.[56] We performed qRT-PCR analysis of genes coding for the small and large subunits of ribosomes, *OsRPS4* and *OsRPL23A*, respectively. Both of these genes showed upregulation upon wounding, and the response was exaggerated in KO and suppressed in OE plants (Figure 6H). Furthermore, to check the extent of cell death upon wounding, we subjected WT, OE, and KO leaves for wounding, followed by staining for cell death using trypan blue. KO leaves showed exaggerated cell death in comparison to WT, whereas this cell death-exhibiting region was restricted in OE (Figure 6I). These observations suggest that OsPSKR possibly assists in the transitioning of responses from early defense to late recovery responses, and such a transition is perturbed in KO (Figure 6F). Perturbation of this transitioning led to exaggerated defense responses, leading to constitutive cell death that is detrimental to growth post-wounding.

OsPSKR and OsPEPR1 displayed mutual antagonism, leading to negative crosstalk between growth and defense signal receptors

We observed that OsPSKR positively influenced wound responses at early time points and negatively impacted late wound responses. Similar regulation has been shown for AtFERONIA, which acts as a scaffold to positively influence immune responses and ligand perception, leading to the attenuation of immune responses by the same protein.[57] We hypothesized that OsPSKR might crosstalk with OsPep3-mediated signaling to assist in signal transitioning post-wounding. It has been shown that OsPEPR1 is involved in Pep signal perception.[58] Therefore, we considered OsPEPR1 to test this possibility. We transiently expressed OsPEPR1 in *N. benthamiana* plants and treated them with both OsPep2 and OsPep3. This resulted in MPK activation, suggesting that OsPEPR1 is the authentic receptor for both peptides, while treatment with OsPep2 or OsPep3 alone did not result in MPK activation (Figure 7A). To check whether OsPSKR is capable of altering OsPEPR1-mediated MPK activation (Figure S7B), we co-expressed OsPSKR and OsPEPR1, followed by Pep3/PSK/Pep3 + PSK treatments. We found that the MPK activation by OsPep3 through OsPEPR1 was reduced irrespective of PSK (Figures 7B, S7C, and S7D). This indicates that OsPSKR negatively impacts signaling mediated by OsPEPR.

We also observed that the co-expression of these two receptors led to mutual reduction in protein levels, suggesting a possible antagonism. Also, the OsPEPR1-induced reduction of OsPSKR was OsPep3 signal dependent (Figures 7B, S7C, and S7D). This indicates the possibility that in rice, upon OsPEPR1 signal activation through OsPep3 post-wounding, OsPSKR is destabilized and excluded from activating its suppressive role on PEPR. Furthermore, it is possible that, when OsPep3-induced signaling subsides, PSK signaling is activated, as seen in transcriptome analysis. OsPROPEP3 was active at 15–30 min post-wounding, while the PSK signal was activated around 2 h, further suggesting mutually exclusive signal activation between these two contrasting signals (Figure 7C). This mutual crosstalk between these two receptors supports the idea of potential temporal signal relay. Furthermore, we checked whether the mutual antagonism between these two receptors is dependent on ubiquitination-mediated 26S proteasomal degradation. We performed these experiments in the presence of MG132, an inhibitor of the 26S proteasomal pathway, and observed partial restoration of both OsPSKR and OsPEPR1 when they were co-expressed (Figures 7D and S7E). The reduction of OsPSKR levels by OsPEPR1 after OsPep3 treatment might be due to the kinase activity of OsPEPR1. To test this, we generated a catalytic activity mutant of OsPEPR1 through site-directed mutagenesis. OsPEPR1ΔKD failed to activate MPK signaling upon OsPep3 treatment, indicating the authenticity of the receptor (Figure 7E). However, co-expression of OsPSKR with OsPEPR1ΔKD failed to restore OsPSKR levels to mock condition upon OsPep3 treatment (Figure 7E). This suggests that the antagonization of OsPSKR by OsPEPR1 is OsPep3 dependent but kinase activity independent, and future mechanistic studies are required to understand this interaction further. Together, these results indicate that OsPEPR1 and OsPSKR mutually exclude each other from signaling, leading to temporally separated signal relay between these pathways, which happens in a Pep3-dependent manner.

Collectively, through this study, we have shown that wounding triggers signal relay between small peptides involved in defense and growth functions. This signal relay activates OsPSKR-mediated signaling, which acts at the nexus of signal transition between early defense and late growth responses (Figure 7F).

DISCUSSION

Wound responses have been investigated mainly in the context of insect herbivory in monocots, and their distinctness from dicots is not very well known. Studies in dicots show that wounding involves signal transition from defense to growth/regeneration responses.[4,5] Monocots usually fail to acquire stem cell ability and lack regeneration abilities post-wounding.[6] The experiments discussed here provide insights into the stepwise molecular signaling events that are a part of the mechanical wounding responses in rice.

Our findings indicate the presence of a signaling cascade mediated by two distinct endogenous peptides in signaling

(F) Schematic showing the role of OsPSKR in signal transitioning from early to late wound responses.
(G) qRT-PCR analysis of *OsNAC4*, *OsNAC2*, and *OsPR4c* post-12 h of wounding relative to *OsActin* in WT and transgenic plants.
(H) qRT-PCR analysis of *OsRPS4* and *OsRPL23A* post-12 h of wounding in WT and transgenic plants; $n = 3$, pairwise Student's t test. $^{*}p < 0.05$; $^{**}p < 0.005$.
(I) Cell death assessment post-wounding in WT, OE, and KO plants. Leaves were subjected to trypan blue staining 48 h post-wounding. Scale bars, 1 mm.
$n = 3$ for all qPCR experiments, error bars indicate SEM, pairwise Student's t test with respect to control samples; $^{*}p < 0.05$; $^{**}p < 0.005$.

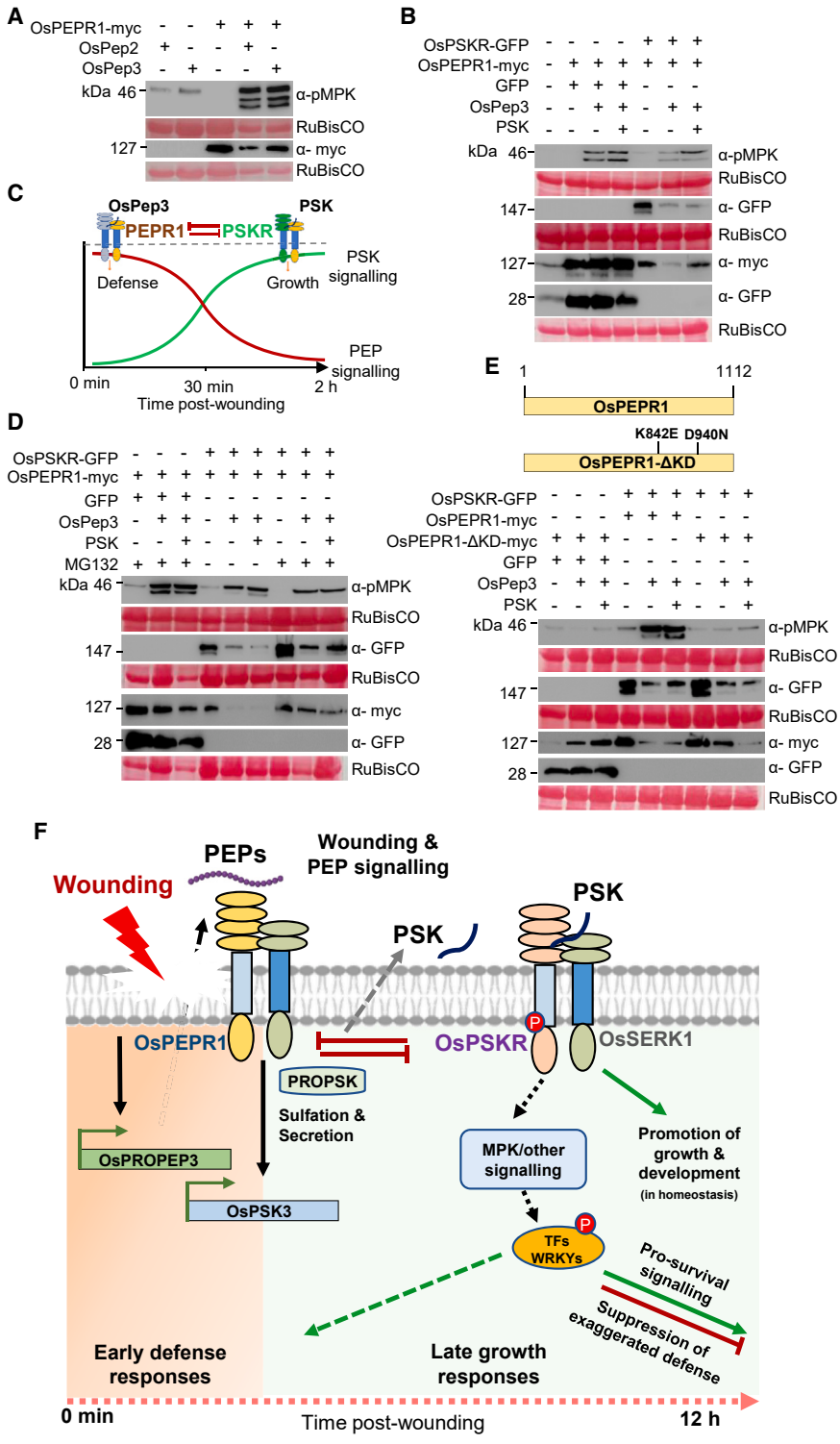

Figure 7. OsPSKR and OsPEPR1 mutually antagonize each other

(A) MPK activation assay depicting MPK activation in the presence of OsPEPR1 expressed transiently.

(B) Co-expression of OsPEPR1 and OsPSKR showing the mutual antagonism between each other in OsPep3-dependent manner.

(C) Schematic showing the temporal signal relay between OsPep3- and PSK-mediated signaling post-wounding.

(D) Co-expression of OsPEPR1 and OsPSKR in the presence of MG132.

(E) Co-expression of OsPEPR1 kinase activity mutant and OsPSKR shows that the antagonization of PSKR is independent of kinase activity of OsPEPR1. All these experiments were performed in *N. benthamiana* plants. Samples were processed 2 days post-infiltration.

(F) Proposed model: wounding and PEP treatment leads to the activation of PSK signaling mediated by OsPSKR. OsPSKR acts at the intersection of transition between defense and growth signaling and acts as a pro-growth signal by assisting in the suppression of exaggerated defense responses, including suppression of OsPEPR1.

wound responses. Very early activation of PEP coding genes upon wounding and its overlapping downstream responses with wounding in rice suggested a strong role for PEP-induced responses. Bioactive peptides derived from PROPEPs possess a conserved stretch of EGxGGxGGxxH at the C terminus and serve as immune triggers across plants (Figure S1B). The spatiotemporal regulation of OsPROPEPs, subcellular localization, and release into extracellular space upon processing need to be investigated further to deduce their distinct roles. Studies in dicots have indicated the presence of a temporal signal relay mediated by phytohormones JA and auxin, which promote wound-induced regeneration.[5,8] Such a signal relay might connect initial defense signals with delayed growth signals. We have observed similar crosstalk between two peptide hormones, OsPep3 and PSK, that might contribute to responses similar to those with JA and auxin.

In *Arabidopsis*, it has been proposed that the crosstalk between brassinosteroid and PSK signaling determines cell fate, leading to procambial cell identity.[59] Although rice and other monocots lack wound-induced regeneration ability, it is possible that the PSK signaling might contribute to wound-induced growth promotion in rice. Our findings reveal OsPSKR as a PSK receptor that was induced post-induction of the PSK precursor upon wounding. These findings might also apply to herbivory and other stress responses where PSK might be involved in signaling.

PSK signaling has been attributed to various growth functions.[25,26,28,59,60] However, the loss of function of PSK receptors

in other species did not lead to drastic phenotypes unlike what was observed here. PSK signaling has important functions in rice development beyond wound responses. Furthermore, the insensitivity of KO plants to PSK treatment emphasized a lack of functional redundancy between other predicted OsPSKRs.

Interestingly, transcriptome analysis of transgenic plants identified many wound-responsive genes under the direct control of OsPSKR-mediated signaling. Callose deposition, one of the early responses to wounding, is also compromised in the case of KO plants upon wounding. It is important to note that callose deposition is also a growth and development-associated process.[61] In *Arabidopsis*, AtABCG36, which is attributed to callose deposition, regulates the transport of both growth- and defense-related metabolites, resulting in the maintenance of growth-defense balance.[62] The transport of distinct metabolites by AtABCG36 depends on the phosphorylation status of the protein that is controlled by an LRR-RLK called QSK1.[62] Compromised expression of the rice homologs of AtABCG36 upon wounding in KO plants suggested a similar mechanism of regulation of ABCG transporters by OsPSKR either directly or indirectly. Unregulated wound responses are detrimental to the fitness of plants and can lead to delayed progression to growth post-wounding. KO plants showed constitutive cell death and ROS accumulation phenotypes, which are suggestive of autoimmune responses, indicating that OsPSKR is a negative regulator of defense responses in homeostasis. Various proteins have been attributed to the regulation of exaggerated defense responses upon wounding. In *Arabidopsis*, BOS1/MYB108 regulates cell death upon wounding, and its mutation leads to exaggerated wound-induced cell death.[63] When defense signaling proteins like glutamate receptors were constitutively activated, plant regeneration post-wounding was compromised.[4] A similar mechanism might be present in rice, where OsPSKR might assist in the promotion of growth post-wounding by suppressing defense. Rapidly shifting to growth phase upon wounding might be a strategy evolved by monocots that interacted with herbivores for millions of years. In *Arabidopsis*, the transcriptional activation of PSK and PSKR upon wounding was much delayed,[27,29] in comparison to rice, as observed here. The positive regulation of early responses and suppression of late wound responses by OsPSKR could simply be attributed to temporal lag in PSK availability, which comes at an intermediary stage between early and late wound responses (Figure 7F). Recent reports suggest that AtFERONIA can assume a scaffolding role in promoting immune responses, and ligand introduction leads to suppression of immune responses.[57] It has also been shown that AtPSYR1, a sulfated peptide-hormone receptor has a ligand-independent role in promoting stress responses and a ligand-dependent role in promoting growth responses.[64] It is possible that OsPSKR, which is also a sulfated peptide-hormone receptor, seems to be playing a similar regulatory role.

Constitutive cell death and ROS accumulation even during homeostasis in KO plants could be due to perturbed ion homeostasis, as observed in the case of mutants of membrane proteins like BAK1 in *Arabidopsis*.[65–67] Deregulation of AtBAK1, a co-receptor for many ligand-binding receptors, including AtPSKR1, led to autoimmune phenotypes. This was due to the perturbation of calcium signaling via CNGC19/20 proteins, hyperactivation of NLR proteins, and released suppression of other LRR-RLKs.[65–67] AtPSKR1 was shown to interact with AtCNGC17 and an ATPase.[68] Activation of cell death phenotypes in OsPSKR KO might be due to the perturbation of membrane components that are involved in their dynamics. This possibility needs to be investigated further. Studies in other plant species have shown the role of PSK receptor in attenuation of plant immunity.[69] The absence of PSK receptor led to autoimmune responses during beneficial microbe interaction by hyperactivating SA signaling.[70] We observed upregulation of SA biosynthesis gene OsICS1 upon wounding in KO, which was otherwise non-responsive to wounding in WT and OE lines, suggesting the de-repression of SA signaling. PSK signaling has also been implicated in maintaining ROS homeostasis.[71] In maize, PSK signaling suppressed cell death during wounding,[72] similar to the observations reported here. PSK signaling also optimized growth defense through distinct phosphorylation of glutamine synthetase GS2 through a calcium-dependent protein kinase.[73,74] All these studies indicated the importance of PSK-PSKR signaling in maintaining growth defense trade-off across various plant species. Our identification of the upstream signaling in PSK signaling and the downstream events in maintaining growth-defense trade-off upon wounding is timely.

Through this study, we uncovered a very important peptide-mediated signal relay responsive to wounding in rice. Such studies can pave the way for a better understanding of general plant responses that operate by relying on endogenous signals. They also might help in dissecting out the responses that are specific to wounding, which are not appreciated in insect herbivore responses. Wounding is not just an adverse reaction akin to pathogenic attack; it also triggers growth and flowering in several horticultural crop plants. Understanding these events and identifying key regulators has implications in improving crop yield.

Limitations of the study

We have provided evidence of PSKR in assisting signal transitioning post-wounding at the gene expression level. Genetic and biochemical evidence to prove the temporal hierarchy using perturbed lines of the genes mentioned here would be essential. Since the KO of PSKR led to sterility, the mechanistic basis of wound response regulation by OsPSKR could not be addressed here. Biochemical evidence in future investigations would be necessary to identify how OsPSKR mediates the suppression of cell death and also to ascertain the nature of the crosstalk with OsPEPR.

STAR★METHODS

Detailed methods are provided in the online version of this paper and include the following:

- KEY RESOURCES TABLE
- RESOURCE AVAILABILITY
  - Lead contact
  - Materials availability
  - Data and code availability
- EXPERIMENTAL MODEL AND STUDY PARTICIPANT DETAILS
  - Plant materials and growth conditions
  - Bacterial strains

- METHOD DETAILS
  - Plasmid construction and cloning
  - Rice transformation
  - Transient expression through *Agrobacterium* infiltration
  - Leaf wounding experiment
  - Peptide treatment
  - RT-qPCR analyses
  - Transcriptome analysis
  - GO analysis
  - Phylogenetic analysis
  - Homology modeling and docking studies
  - Molecular dynamics (MD) simulation study
  - Southern blotting
  - sRNA northern protocol
  - Recombinant protein expression and purification
  - MPK activation assay
  - MST assay
  - *In vitro* protein kinase assay
  - Protein extraction, immunoblotting and IP
  - SEM imaging and micro-computed tomography (micro CT)
  - Pollen staining
  - DAB staining
  - Trypan blue staining
  - Callose staining and imaging
- QUANTIFICATION AND STATISTICAL ANALYSIS

SUPPLEMENTAL INFORMATION

Supplemental information can be found online at https://doi.org/10.1016/j.celrep.2024.114515.

ACKNOWLEDGMENTS

We thank the members of the Shivaprasad lab for suggestions. We thank the next-generation genomics, Radiation, Central Imaging & Flow Cytometry Facility, Centre for Chemical Biology and Therapeutics (CCBT)-inStem, and electron microscopy facilities at the National Centre for Biological Sciences/Tata Institute of Fundamental Research, Bangalore. We thank K. Veluthambi for binary vectors, PB1 seeds, and *Agrobacterium* strains. We thank Vikrant (CCBT) for helping out with the MST experiments. This study was supported by the Department of Atomic Energy, Government of India, under project identification no. RTI 4006 (1303/3/2019/R&D-II/DAE/4749, dated July 16, 2020). This work was also supported by grant no. BT/IN/Swiss/47/JGK/2018-19 from the Department of Biotechnology and MST/PRAO/Control/2020-21/PFMS from the Department of Science and Technology, Government of India.

AUTHOR CONTRIBUTIONS

C.Y.H. and P.V.S. conceptualized the study, analyzed the data, and wrote the manuscript. C.Y.H. performed most of the experiments. A.P. performed the SEM imaging. A.N. helped in the kinase assay. M.C. performed the modeling and docking. S.R. performed the confocal imaging.

DECLARATION OF INTERESTS

The authors declare no competing interests.

Received: August 3, 2023
Revised: May 13, 2024
Accepted: July 1, 2024
Published: July 13, 2024

REFERENCES

1. Engelsdorf, T., Gigli-Bisceglia, N., Veerabagu, M., McKenna, J.F., Vaahtera, L., Augstein, F., Van der Does, D., Zipfel, C., and Hamann, T. (2018). The plant cell wall integrity maintenance and immune signaling systems cooperate to control stress responses in Arabidopsis thaliana. Sci. Signal. *11*, eaao3070. https://doi.org/10.1126/scisignal.aao3070.
2. Vega-Muñoz, I., Duran-Flores, D., Fernández-Fernández, Á.D., Heyman, J., Ritter, A., and Stael, S. (2020). Breaking bad news: Dynamic molecular mechanisms of wound response in plants. Front. Plant Sci. *11*, 610445. https://doi.org/10.3389/fpls.2020.610445.
3. Savatin, D.V., Gramegna, G., Modesti, V., and Cervone, F. (2014). Wounding in the plant tissue: the defense of a dangerous passage. Front. Plant Sci. *5*, 470. https://doi.org/10.3389/fpls.2014.00470.
4. Hernández-Coronado, M., Dias Araujo, P.C., Ip, P.-L., Nunes, C.O., Rahni, R., Wudick, M.M., Lizzio, M.A., Feijó, J.A., and Birnbaum, K.D. (2022). Plant glutamate receptors mediate a bet-hedging strategy between regeneration and defense. Dev. Cell *57*, 451–465.e6. https://doi.org/10.1016/j.devcel.2022.01.013.
5. Zhang, G., Zhao, F., Chen, L., Pan, Y., Sun, L., Bao, N., Zhang, T., Cui, C.-X., Qiu, Z., Zhang, Y., et al. (2019). Jasmonate-mediated wound signalling promotes plant regeneration. Nat. Plants *5*, 491–497. https://doi.org/10.1038/s41477-019-0408-x.
6. Liang, Y., Heyman, J., Lu, R., and De Veylder, L. (2023). Evolution of wound-activated regeneration pathways in the plant kingdom. Eur. J. Cell Biol. *102*, 151291. https://doi.org/10.1016/j.ejcb.2023.151291.
7. Hu, B., Zhang, G., Liu, W., Shi, J., Wang, H., Qi, M., Li, J., Qin, P., Ruan, Y., Huang, H., et al. (2017). Divergent regeneration-competent cells adopt a common mechanism for callus initiation in angiosperms. Regeneration (Oxf.) *4*, 132–139. https://doi.org/10.1002/reg2.82.
8. Radhakrishnan, D., Shanmukhan, A.P., Kareem, A., Aiyaz, M., Varapparambathu, V., Toms, A., Kerstens, M., Valsakumar, D., Landge, A.N., Shaji, A., et al. (2020). A coherent feed-forward loop drives vascular regeneration in damaged aerial organs of plants growing in a normal developmental context. Development *147*, dev185710. https://doi.org/10.1242/dev.185710.
9. Erb, M., and Reymond, P. (2019). Molecular interactions between plants and insect herbivores. Annu. Rev. Plant Biol. *70*, 527–557. https://doi.org/10.1146/annurev-arplant-050718-095910.
10. Tavormina, P., De Coninck, B., Nikonorova, N., De Smet, I., and Cammue, B.P.A. (2015). The plant peptidome: An expanding repertoire of structural features and biological functions. Plant Cell *27*, 2095–2118. https://doi.org/10.1105/tpc.15.00440.
11. Li, Q., Wang, C., and Mou, Z. (2020). Perception of damaged self in plants. Plant Physiol. *182*, 1545–1565. https://doi.org/10.1104/pp.19.01242.
12. Tanaka, K., and Heil, M. (2021). Damage-associated molecular patterns (DAMPs) in plant innate immunity: Applying the danger model and evolutionary perspectives. Annu. Rev. Phytopathol. *59*, 53–75. https://doi.org/10.1146/annurev-phyto-082718-100146.
13. Huffaker, A., Pearce, G., and Ryan, C.A. (2006). An endogenous peptide signal in Arabidopsis activates components of the innate immune response. Proc. Natl. Acad. Sci. USA *103*, 10098–10103. https://doi.org/10.1073/pnas.0603727103.
14. Pearce, G., Strydom, D., Johnson, S., and Ryan, C.A. (1991). A polypeptide from tomato leaves induces wound-inducible proteinase inhibitor proteins. Science *253*, 895–897. https://doi.org/10.1126/science.253.5022.895.
15. Ryan, C.A., and Pearce, G. (1998). Systemin: a polypeptide signal for plant defensive genes. Annu. Rev. Cell Dev. Biol. *14*, 1–17. https://doi.org/10.1146/annurev.cellbio.14.1.1.
16. Shinya, T., Yasuda, S., Hyodo, K., Tani, R., Hojo, Y., Fujiwara, Y., Hiruma, K., Ishizaki, T., Fujita, Y., Saijo, Y., and Galis, I. (2018). Integration of danger peptide signals with herbivore-associated molecular pattern signaling amplifies anti-herbivore defense responses in rice. Plant J. *94*, 626–637. https://doi.org/10.1111/tpj.13883.
17. Huffaker, A., Dafoe, N.J., and Schmelz, E.A. (2011). ZmPep1, an ortholog of Arabidopsis elicitor peptide 1, regulates maize innate immunity and

enhances disease resistance. Plant Physiol. *155*, 1325–1338. https://doi.org/10.1104/pp.110.166710.

18. Huffaker, A., Pearce, G., Veyrat, N., Erb, M., Turlings, T.C.J., Sartor, R., Shen, Z., Briggs, S.P., Vaughan, M.M., Alborn, H.T., et al. (2013). Plant elicitor peptides are conserved signals regulating direct and indirect antiherbivore defense. Proc. Natl. Acad. Sci. USA *110*, 5707–5712. https://doi.org/10.1073/pnas.1214668110.
19. Lori, M., van Verk, M.C., Hander, T., Schatowitz, H., Klauser, D., Flury, P., Gehring, C.A., Boller, T., and Bartels, S. (2015). Evolutionary divergence of the plant elicitor peptides (Peps) and their receptors: interfamily incompatibility of perception but compatibility of downstream signalling. J. Exp. Bot. *66*, 5315–5325. https://doi.org/10.1093/jxb/erv236.
20. Trivilin, A.P., Hartke, S., and Moraes, M.G. (2014). Components of different signalling pathways regulated by a new orthologue of <scp>A</scp>t<scp>PROPEP</scp>1 in tomato following infection by pathogens. Plant Pathol. *63*, 1110–1118. https://doi.org/10.1111/ppa.12190.
21. Poretsky, E., Dressano, K., Weckwerth, P., Ruiz, M., Char, S.N., Shi, D., Abagyan, R., Yang, B., and Huffaker, A. (2020). Differential activities of maize plant elicitor peptides as mediators of immune signaling and herbivore resistance. Plant J. *104*, 1582–1602. https://doi.org/10.1111/tpj.15022.
22. Bartels, S., Lori, M., Mbengue, M., van Verk, M., Klauser, D., Hander, T., Böni, R., Robatzek, S., and Boller, T. (2013). The family of Peps and their precursors in Arabidopsis: differential expression and localization but similar induction of pattern-triggered immune responses. J. Exp. Bot. *64*, 5309–5321. https://doi.org/10.1093/jxb/ert330.
23. Bjornson, M., Pimprikar, P., Nürnberger, T., and Zipfel, C. (2021). The transcriptional landscape of Arabidopsis thaliana pattern-triggered immunity. Nat. Plants *7*, 579–586. https://doi.org/10.1038/s41477-021-00874-5.
24. Motomitsu, A., Sawa, S., and Ishida, T. (2015). Plant peptide hormone signalling. Essays Biochem. *58*, 115–131. https://doi.org/10.1042/bse0580115.
25. Matsubayashi, Y., and Sakagami, Y. (1996). Phytosulfokine, sulfated peptides that induce the proliferation of single mesophyll cells of Asparagus officinalis L. Proc. Natl. Acad. Sci. USA *93*, 7623–7627. https://doi.org/10.1073/pnas.93.15.7623.
26. Matsubayashi, Y., Takagi, L., Omura, N., Morita, A., and Sakagami, Y. (1999). The endogenous sulfated pentapeptide phytosulfokine-α stimulates tracheary element differentiation of isolated mesophyll cells of zinnia. Plant Physiol. *120*, 1043–1048. https://doi.org/10.1104/pp.120.4.1043.
27. Matsubayashi, Y., Ogawa, M., Kihara, H., Niwa, M., and Sakagami, Y. (2006). Disruption and overexpression of Arabidopsis phytosulfokine receptor gene affects cellular longevity and potential for growth. Plant Physiol. *142*, 45–53. https://doi.org/10.1104/pp.106.081109.
28. Sauter, M. (2015). Phytosulfokine peptide signalling. J. Exp. Bot. *66*, 5161–5169. https://doi.org/10.1093/jxb/erv071.
29. Loivamäki, M., Stührwohldt, N., Deeken, R., Steffens, B., Roitsch, T., Hedrich, R., and Sauter, M. (2010). A role for PSK signaling in wounding and microbial interactions in Arabidopsis. Physiol. Plantarum *139*, 348–357. https://doi.org/10.1111/j.1399-3054.2010.01371.x.
30. Wang, J., Li, H., Han, Z., Zhang, H., Wang, T., Lin, G., Chang, J., Yang, W., and Chai, J. (2015). Allosteric receptor activation by the plant peptide hormone phytosulfokine. Nature *525*, 265–268. https://doi.org/10.1038/nature14858.
31. Zhang, H., Hu, Z., Lei, C., Zheng, C., Wang, J., Shao, S., Li, X., Xia, X., Cai, X., Zhou, J., et al. (2018). A plant phytosulfokine peptide initiates auxin-dependent immunity through cytosolic Ca2+ signaling in tomato. Plant Cell *30*, 652–667. https://doi.org/10.1105/tpc.17.00537.
32. Hohmann, U., Lau, K., and Hothorn, M. (2017). The structural basis of ligand perception and signal activation by receptor kinases. Annu. Rev. Plant Biol. *68*, 109–137. https://doi.org/10.1146/annurev-arplant-042916-040957.
33. Matsubayashi, Y., Ogawa, M., Morita, A., and Sakagami, Y. (2002). An LRR receptor kinase involved in perception of a peptide plant hormone, phytosulfokine. Science *296*, 1470–1472. https://doi.org/10.1126/science.1069607.
34. Nagar, P., Kumar, A., Jain, M., Kumari, S., and Mustafiz, A. (2020). Genome-wide analysis and transcript profiling of PSKR gene family members in Oryza sativa. PLoS One *15*, e0236349. https://doi.org/10.1371/journal.pone.0236349.
35. Yang, W., Zhang, B., Qi, G., Shang, L., Liu, H., Ding, X., and Chu, Z. (2019). Identification of the phytosulfokine receptor 1 (OsPSKR1) confers resistance to bacterial leaf streak in rice. Planta *250*, 1603–1612. https://doi.org/10.1007/s00425-019-03238-8.
36. Nagar, P., Sharma, N., Jain, M., Sharma, G., Prasad, M., and Mustafiz, A. (2022). OsPSKR15, a phytosulfokine receptor from rice enhances abscisic acid response and drought stress tolerance. Physiol. Plantarum *174*, e13569. https://doi.org/10.1111/ppl.13569.
37. Venu, R.C., Sheshu Madhav, M., Sreerekha, M.V., Nobuta, K., Zhang, Y., Carswell, P., Boehm, M.J., Meyers, B.C., Korth, K.L., and Wang, G.-L. (2010). Deep and comparative transcriptome analysis of rice plants infested by the beet armyworm (Spodoptera exigua) and water weevil (Lissorhoptrus oryzophilus). Rice *3*, 22–35. https://doi.org/10.1007/s12284-010-9037-8.
38. Hari Sundar, G.,V., Swetha, C., Basu, D., Pachamuthu, K., Raju, S., Chakraborty, T., Mosher, R.A., and Shivaprasad, P.V. (2023). Plant polymerase IV sensitizes chromatin through histone modifications to preclude spread of silencing into protein-coding domains. Genome Res. *33*, 715–728. https://doi.org/10.1101/gr.277353.122.
39. Nomoto, M., Skelly, M.J., Itaya, T., Mori, T., Suzuki, T., Matsushita, T., Tokizawa, M., Kuwata, K., Mori, H., Yamamoto, Y.Y., et al. (2021). Suppression of MYC transcription activators by the immune cofactor NPR1 fine-tunes plant immune responses. Cell Rep. *37*, 110125. https://doi.org/10.1016/j.celrep.2021.110125.
40. Tost, A.S., Kristensen, A., Olsen, L.I., Axelsen, K.B., and Fuglsang, A.T. (2021). The PSY peptide family-expression, modification and physiological implications. Genes *12*, 218. https://doi.org/10.3390/genes12020218.
41. Sharma, A., Hussain, A., Mun, B.-G., Imran, Q.M., Falak, N., Lee, S.-U., Kim, J.Y., Hong, J.K., Loake, G.J., Ali, A., and Yun, B.W. (2016). Comprehensive analysis of plant rapid alkalization factor (RALF) genes. Plant Physiol. Biochem. *106*, 82–90. https://doi.org/10.1016/j.plaphy.2016.03.037.
42. Zheng, X., Kang, S., Jing, Y., Ren, Z., Li, L., Zhou, J.-M., Berkowitz, G., Shi, J., Fu, A., Lan, W., et al. (2018). Danger-associated peptides close stomata by OST1-independent activation of anion channels in guard cells. Plant Cell *30*, 1132–1146. https://doi.org/10.1105/tpc.17.00701.
43. Hu, L., Ye, M., Kuai, P., Ye, M., Erb, M., and Lou, Y. (2018). OsLRR-RLK1, an early responsive leucine-rich repeat receptor-like kinase, initiates rice defense responses against a chewing herbivore. New Phytol. *219*, 1097–1111. https://doi.org/10.1111/nph.15247.
44. DeFalco, T.A., and Zipfel, C. (2021). Molecular mechanisms of early plant pattern-triggered immune signaling. Mol. Cell *81*, 3449–3467. https://doi.org/10.1016/j.molcel.2021.07.029.
45. Shiu, S.-H., Karlowski, W.M., Pan, R., Tzeng, Y.-H., Mayer, K.F.X., and Li, W.-H. (2004). Comparative analysis of the receptor-like kinase family in Arabidopsis and rice. Plant Cell *16*, 1220–1234. https://doi.org/10.1105/tpc.020834.
46. Wang, X., Kota, U., He, K., Blackburn, K., Li, J., Goshe, M.B., Huber, S.C., and Clouse, S.D. (2008). Sequential transphosphorylation of the BRI1/BAK1 receptor kinase complex impacts early events in brassinosteroid signaling. Dev. Cell *15*, 220–235. https://doi.org/10.1016/j.devcel.2008.06.011.

47. Bender, K.W., Couto, D., Kadota, Y., Macho, A.P., Sklenar, J., Derbyshire, P., Bjornson, M., DeFalco, T.A., Petriello, A., Font Farre, M., et al. (2021). Activation loop phosphorylation of a non-RD receptor kinase initiates plant innate immune signaling. Proc. Natl. Acad. Sci. USA *118*, e2108242118. https://doi.org/10.1073/pnas.2108242118.

48. Ma, X., Xu, G., He, P., and Shan, L. (2016). SERKing coreceptors for receptors. Trends Plant Sci. *21*, 1017–1033. https://doi.org/10.1016/j.tplants.2016.08.014.

49. Ossowski, S., Schwab, R., and Weigel, D. (2008). Gene silencing in plants using artificial microRNAs and other small RNAs. Plant J. *53*, 674–690. https://doi.org/10.1111/j.1365-313X.2007.03328.x.

50. Schwab, R., Ossowski, S., Riester, M., Warthmann, N., and Weigel, D. (2006). Highly specific gene silencing by artificial microRNAs in Arabidopsis. Plant Cell *18*, 1121–1133. https://doi.org/10.1105/tpc.105.039834.

51. Narjala, A., Nair, A., Tirumalai, V., Hari Sundar, G.V., and Shivaprasad, P.V. (2020). A conserved sequence signature is essential for robust plant miRNA biogenesis. Nucleic Acids Res. *48*, 3103–3118. https://doi.org/10.1093/nar/gkaa077.

52. Matern, A., Böttcher, C., Eschen-Lippold, L., Westermann, B., Smolka, U., Döll, S., Trempel, F., Aryal, B., Scheel, D., Geisler, M., and Rosahl, S. (2019). A substrate of the ABC transporter PEN3 stimulates bacterial flagellin (flg22)-induced callose deposition in Arabidopsis thaliana. J. Biol. Chem. *294*, 6857–6870. https://doi.org/10.1074/jbc.RA119.007676.

53. Pandey, B.K., Verma, L., Prusty, A., Singh, A.P., Bennett, M.J., Tyagi, A.K., Giri, J., and Mehra, P. (2021). OsJAZ11 regulates phosphate starvation responses in rice. Planta *254*, 8. https://doi.org/10.1007/s00425-021-03657-6.

54. Kaneda, T., Taga, Y., Takai, R., Iwano, M., Matsui, H., Takayama, S., Isogai, A., and Che, F.-S. (2009). The transcription factor OsNAC4 is a key positive regulator of plant hypersensitive cell death. EMBO J. *28*, 926–936. https://doi.org/10.1038/emboj.2009.39.

55. Mao, C., Ding, J., Zhang, B., Xi, D., and Ming, F. (2018). OsNAC2 positively affects salt-induced cell death and binds to the OsAP37 and OsCOX11 promoters. Plant J. *94*, 454–468. https://doi.org/10.1111/tpj.13867.

56. Zhou, Y., Niu, R., Tang, Z., Mou, R., Wang, Z., Zhu, S., Yang, H., Ding, P., and Xu, G. (2023). Plant HEM1 specifies a condensation domain to control immune gene translation. Nat. Plants *9*, 289–301. https://doi.org/10.1038/s41477-023-01355-7.

57. Stegmann, M., Monaghan, J., Smakowska-Luzan, E., Rovenich, H., Lehner, A., Holton, N., Belkhadir, Y., and Zipfel, C. (2017). The receptor kinase FER is a RALF-regulated scaffold controlling plant immune signaling. Science *355*, 287–289. https://doi.org/10.1126/science.aal2541.

58. Shen, W., Zhang, X., Liu, J., Tao, K., Li, C., Xiao, S., Zhang, W., and Li, J.-F. (2022). Plant elicitor peptide signalling confers rice resistance to piercing-sucking insect herbivores and pathogens. Plant Biotechnol. J. *20*, 991–1005. https://doi.org/10.1111/pbi.13781.

59. Holzwart, E., Huerta, A.I., Glöckner, N., Garnelo Gómez, B., Wanke, F., Augustin, S., Askani, J.C., Schürholz, A.-K., Harter, K., and Wolf, S. (2018). BRI1 controls vascular cell fate in the Arabidopsis root through RLP44 and phytosulfokine signaling. Proc. Natl. Acad. Sci. USA *115*, 11838–11843. https://doi.org/10.1073/pnas.1814434115.

60. Stührwohldt, N., Dahlke, R.I., Kutschmar, A., Peng, X., Sun, M.-X., and Sauter, M. (2015). Phytosulfokine peptide signaling controls pollen tube growth and funicular pollen tube guidance in Arabidopsis thaliana. Physiol. Plantarum *153*, 643–653. https://doi.org/10.1111/ppl.12270.

61. Wang, B., Andargie, M., and Fang, R. (2022). The function and biosynthesis of callose in high plants. Heliyon *8*, e09248. https://doi.org/10.1016/j.heliyon.2022.e09248.

62. Aryal, B., Xia, J., Hu, Z., Stumpe, M., Tsering, T., Liu, J., Huynh, J., Fukao, Y., Glöckner, N., Huang, H.-Y., et al. (2023). An LRR receptor kinase controls ABC transporter substrate preferences during plant growth-defense decisions. Curr. Biol. *33*, 2008–2023.e8. https://doi.org/10.1016/j.cub.2023.04.029.

63. Cui, F., Brosché, M., Sipari, N., Tang, S., and Overmyer, K. (2013). Regulation of ABA dependent wound induced spreading cell death by MYB108. New Phytol. *200*, 634–640. https://doi.org/10.1111/nph.12456.

64. Ogawa-Ohnishi, M., Yamashita, T., Kakita, M., Nakayama, T., Ohkubo, Y., Hayashi, Y., Yamashita, Y., Nomura, T., Noda, S., Shinohara, H., and Matsubayashi, Y. (2022). Peptide ligand-mediated trade-off between plant growth and stress response. Science *378*, 175–180. https://doi.org/10.1126/science.abq5735.

65. Yu, X., Xu, G., Li, B., de Souza Vespoli, L., Liu, H., Moeder, W., Chen, S., de Oliveira, M.V.V., Ariádina de Souza, S., Shao, W., et al. (2019). The receptor kinases BAK1/SERK4 regulate Ca2+ channel-mediated cellular homeostasis for cell death containment. Curr. Biol. *29*, 3778–3790.e8. https://doi.org/10.1016/j.cub.2019.09.018.

66. Wu, Y., Gao, Y., Zhan, Y., Kui, H., Liu, H., Yan, L., Kemmerling, B., Zhou, J.-M., He, K., and Li, J. (2020). Loss of the common immune coreceptor BAK1 leads to NLR-dependent cell death. Proc. Natl. Acad. Sci. USA *117*, 27044–27053. https://doi.org/10.1073/pnas.1915339117.

67. Yu, X., Xie, Y., Luo, D., Liu, H., de Oliveira, M.V.V., Qi, P., Kim, S.-I., Ortiz-Morea, F.A., Liu, J., Chen, Y., et al. (2023). A phospho-switch constrains BTL2-mediated phytocytokine signaling in plant immunity. Cell *186*, 2329–2344.e20. https://doi.org/10.1016/j.cell.2023.04.027.

68. Ladwig, F., Dahlke, R.I., Stührwohldt, N., Hartmann, J., Harter, K., and Sauter, M. (2015). Phytosulfokine regulates growth in Arabidopsis through a response module at the plasma membrane that includes CYCLIC NUCLEOTIDE-GATED CHANNEL17, H+-ATPase, and BAK1. Plant Cell *27*, 1718–1729. https://doi.org/10.1105/tpc.15.00306.

69. Igarashi, D., Tsuda, K., and Katagiri, F. (2012). The peptide growth factor, phytosulfokine, attenuates pattern-triggered immunity. Plant J. *71*, 194–204. https://doi.org/10.1111/j.1365-313X.2012.04950.x.

70. Song, S., Morales Moreira, Z., Briggs, A.L., Zhang, X.-C., Diener, A.C., and Haney, C.H. (2023). PSKR1 balances the plant growth-defence trade-off in the rhizosphere microbiome. Nat. Plants *9*, 2071–2084. https://doi.org/10.1038/s41477-023-01539-1.

71. Hao, Z., Wu, H., Zheng, R., Li, R., Zhu, Z., Chen, Y., Lu, Y., Cheng, T., Shi, J., and Chen, J. (2023). The plant peptide hormone phytosulfokine promotes somatic embryogenesis by maintaining redox homeostasis in Cunninghamia lanceolata. Plant J. *113*, 716–733. https://doi.org/10.1111/tpj.16077.

72. Koenig, M., Moser, D., Leusner, J., Depotter, J.R.L., Doehlemann, G., and Villamil, J.M. (2023). Maize phytocytokines modulate pro-survival host responses and pathogen resistance. Mol. Plant Microbe Interact. *36*, 592–604. https://doi.org/10.1094/MPMI-01-23-0005-R.

73. Ding, S., Lv, J., Hu, Z., Wang, J., Wang, P., Yu, J., Foyer, C.H., and Shi, K. (2023). Phytosulfokine peptide optimizes plant growth and defense via glutamine synthetase GS2 phosphorylation in tomato. EMBO J. *42*, e111858. https://doi.org/10.15252/embj.2022111858.

74. Förderer, A., and Chai, J. (2023). Die another day: phytosulfokine at the molecular trade-off between growth and defense in plants. EMBO J. *42*, e113540. https://doi.org/10.15252/embj.2023113540.

75. Xie, K., Minkenberg, B., and Yang, Y. (2015). Boosting CRISPR/Cas9 multiplex editing capability with the endogenous tRNA-processing system. Proc. Natl. Acad. Sci. USA *112*, 3570–3575. https://doi.org/10.1073/pnas.1420294112.

76. Sridevi, G., Sabapathi, N., Meena, P., Nandakumar, R., Samiyappan, R., Muthukrishnan, S., and Veluthambi, K. (2003). Transgenic indica rice variety Pusa basmati 1 constitutively expressing a rice chitinase gene exhibits enhanced resistance to Rhizoctonia solani. J. Plant Biochem. Biotechnol. *12*, 93–101. https://doi.org/10.1007/bf03263168.

77. Swetha, C., Basu, D., Pachamuthu, K., Tirumalai, V., Nair, A., Prasad, M., and Shivaprasad, P.V. (2018). Major domestication-related phenotypes in Indica rice are due to loss of miRNA-mediated laccase silencing. Plant Cell *30*, 2649–2662. https://doi.org/10.1105/tpc.18.00472.

78. Nair, A., Harshith, C.Y., Narjala, A., and Shivaprasad, P.V. (2023). Begomoviral βC1 orchestrates organellar genomic instability to augment viral infection. Plant J. *114*, 934–950. https://doi.org/10.1111/tpj.16186.

79. Schwessinger, B., Bahar, O., Thomas, N., Holton, N., Nekrasov, V., Ruan, D., Canlas, P.E., Daudi, A., Petzold, C.J., Singan, V.R., et al. (2015). Transgenic expression of the dicotyledonous pattern recognition receptor EFR in rice leads to ligand-dependent activation of defense responses. PLoS Pathog. *11*, e1004809. https://doi.org/10.1371/journal.ppat.1004809.

80. Bolger, A.M., Lohse, M., and Usadel, B. (2014). Trimmomatic: a flexible trimmer for Illumina sequence data. Bioinformatics *30*, 2114–2120. https://doi.org/10.1093/bioinformatics/btu170.

81. Kim, D., Langmead, B., and Salzberg, S.L. (2015). HISAT: a fast spliced aligner with low memory requirements. Nat. Methods *12*, 357–360. https://doi.org/10.1038/nmeth.3317.

82. Trapnell, C., Roberts, A., Goff, L., Pertea, G., Kim, D., Kelley, D.R., Pimentel, H., Salzberg, S.L., Rinn, J.L., and Pachter, L. (2014). Erratum: Corrigendum: Differential gene and transcript expression analysis of RNA-seq experiments with TopHat and Cufflinks. Nat. Protoc. *9*, 2513. https://doi.org/10.1038/nprot1014-2513a.

83. Tamura, K., Stecher, G., Peterson, D., Filipski, A., and Kumar, S. (2013). MEGA6: Molecular Evolutionary Genetics Analysis version 6.0. Mol. Biol. Evol. *30*, 2725–2729. https://doi.org/10.1093/molbev/mst197.

84. Sali, A., and Blundell, T.L. (1993). Comparative protein modelling by satisfaction of spatial restraints. J. Mol. Biol. *234*, 779–815. https://doi.org/10.1006/jmbi.1993.1626.

85. Laskowski, R.A., MacArthur, M.W., Moss, D.S., and Thornton, J.M. (1993). PROCHECK: a program to check the stereochemical quality of protein structures. J. Appl. Crystallogr. *26*, 283–291. https://doi.org/10.1107/s0021889892009944.

86. Colovos, C., and Yeates, T.O. (1993). Verification of protein structures: patterns of nonbonded atomic interactions. Protein Sci. *2*, 1511–1519. https://doi.org/10.1002/pro.5560020916.

87. Eisenberg, D., Lüthy, R., and Bowie, J.U. (1997). VERIFY3D: assessment of protein models with three-dimensional profiles. Methods Enzymol. *277*, 396–404. https://doi.org/10.1016/s0076-6879(97)77022-8.

88. Pettersen, E.F., Goddard, T.D., Huang, C.C., Meng, E.C., Couch, G.S., Croll, T.I., Morris, J.H., and Ferrin, T.E. (2021). UCSF ChimeraX: Structure visualization for researchers, educators, and developers. Protein Sci. *30*, 70–82. https://doi.org/10.1002/pro.3943.

89. O'Boyle, N.M., Banck, M., James, C.A., Morley, C., Vandermeersch, T., and Hutchison, G.R. (2011). Open Babel: An open chemical toolbox. J. Cheminf. *3*, 33. https://doi.org/10.1186/1758-2946-3-33.

90. Ghosh, A., Chakraborty, M., Chandra, A., and Alam, M.P. (2021). Structure-activity relationship (SAR) and molecular dynamics study of withaferin-A fragment derivatives as potential therapeutic lead against main protease (Mpro) of SARS-CoV-2. J. Mol. Model. *27*, 97. https://doi.org/10.1007/s00894-021-04703-6.

91. Morris, G.M., Huey, R., Lindstrom, W., Sanner, M.F., Belew, R.K., Goodsell, D.S., and Olson, A.J. (2009). AutoDock4 and AutoDockTools4: Automated docking with selective receptor flexibility. J. Comput. Chem. *30*, 2785–2791. https://doi.org/10.1002/jcc.21256.

92. Shaw, D.E., Dror, R.O., Salmon, J.K., Grossman, J.P., Mackenzie, K.M., Bank, J.A., Young, C., Deneroff, M.M., Batson, B., Bowers, K.J., et al. (2009). Millisecond-scale molecular dynamics simulations on Anton. In Proceedings of the Conference on High Performance Computing Networking, Storage and Analysis (ACM). https://doi.org/10.1145/1654059.1654126.

93. Pachamuthu, K., Hari Sundar, V., Narjala, A., Singh, R.R., Das, S., Avik Pal, H.C.Y., and Shivaprasad, P.V. (2022). Nitrate-dependent regulation of miR444-OsMADS27 signalling cascade controls root development in rice. J. Exp. Bot. *73*, 3511–3530. https://doi.org/10.1093/jxb/erac083.

94. Rogers, S.O., and Bendich, A.J. (1989). Extraction of DNA from plant tissues. In Plant Molecular Biology Manual (Springer Netherlands), pp. 73–83. https://doi.org/10.1007/978-94-009-0951-9_6.

95. Shivaprasad, P.V., Chen, H.-M., Patel, K., Bond, D.M., Santos, B.A.C.M., and Baulcombe, D.C. (2012). A microRNA superfamily regulates nucleotide binding site-leucine-rich repeats and other mRNAs. Plant Cell *24*, 859–874. https://doi.org/10.1105/tpc.111.095380.

96. Hartmann, J., Fischer, C., Dietrich, P., and Sauter, M. (2014). Kinase activity and calmodulin binding are essential for growth signaling by the phytosulfokine receptor PSKR1. Plant J. *78*, 192–202. https://doi.org/10.1111/tpj.12460.

97. Yang, Y., Kim, N.H., Cevik, V., Jacob, P., Wan, L., Furzer, O.J., and Dangl, J.L. (2022). Allelic variation in the Arabidopsis TNL CHS3/CSA1 immune receptor pair reveals two functional cell-death regulatory modes. Cell Host Microbe *30*, 1701–1716.e5. https://doi.org/10.1016/j.chom.2022.09.013.

98. Nair, A., Chatterjee, K.S., Jha, V., Das, R., and Shivaprasad, P.V. (2020). Stability of Begomoviral pathogenicity determinant βC1 is modulated by mutually antagonistic SUMOylation and SIM interactions. BMC Biol. *18*, 110. https://doi.org/10.1186/s12915-020-00843-y.

99. Pachamuthu, K., Swetha, C., Basu, D., Das, S., Singh, I., Sundar, V.H., Sujith, T.N., and Shivaprasad, P.V. (2021). Rice-specific Argonaute 17 controls reproductive growth and yield-associated phenotypes. Plant Mol. Biol. *105*, 99–114. https://doi.org/10.1007/s11103-020-01071-2.

100. Melvin, P., Bankapalli, K., D'Silva, P., and Shivaprasad, P.V. (2017). Methylglyoxal detoxification by a DJ-1 family protein provides dual abiotic and biotic stress tolerance in transgenic plants. Plant Mol. Biol. *94*, 381–397. https://doi.org/10.1007/s11103-017-0613-9.

101. Scalschi, L., Llorens, E., Camaes, G., Pastor, V., Fernndez-Crespo, E., Flors, V., Garca-Agustn, P., and Vicedo, B. (2015). Quantification of callose deposition in plant leaves. Bio Protoc. *5*, e1610. https://doi.org/10.21769/bioprotoc.1610.

STAR★METHODS

KEY RESOURCES TABLE

REAGENT or RESOURCE	SOURCE	IDENTIFIER
Antibodies		
Phospho-p44/42 MAPK (Erk1/2) (Thr202/Tyr204)	CST	Cat: 9101; RRID:AB_331646
Anti-GFP, N-terminal antibody	Sigma	Cat: G1544; RRID:AB_439690
HA-Tag (C29F4) Rabbit mAb	CST	Cat: 3724; RRID:AB_1549585
Anti-Myc tag antibody	Abcam	Cat: ab9106; RRID:AB_307014
Anti-rabbit IgG, HRP-linked Antibody	CST	Cat: 7074; RRID:AB_2099233
Bacterial and virus strains		
Escherichia coli DH5	Prof. K Veluthambi's lab, MKU, India	N/A
Escherichia coli Rosetta-gami	Novagen	71351
Escherichia coli Codon plus	Agilent	230280
Agrobacterium tumefaciens LBA4404 (with pSB1)	Prof. K Veluthambi's lab	N/A
Agrobacterium tumefaciens GV3101	Prof. K Veluthambi's lab	N/A
Chemicals, peptides, and recombinant proteins		
MG132, Proteasome inhibitor	Cellagen technology	Cat: C6413-5
GFP-Trap Magnetic Agarose	Chromotek	Cat: gtma20
Aniline Blue diammonium salt	Sigma	Cat: 415049
Trypan blue	Sigma	Cat: T6146
DAB	Sigma	Cat: D8001
Propidium iodide	Sigma	Cat: P4170
DAPI	Sigma	Cat: D9542
TRIzol	Invitrogen	Cat: 15596018
cOmplete™ Protease Inhibitor Cocktail	Merck	Cat: 11836145001
PMSF	Merck	Cat: 10837091001
DTT	Merck	Cat: 10197777001
OsPep1 peptide	Lifetein	N/A
OsPep2 peptide	Lifetein	N/A
OsPep3 peptide	Lifetein	N/A
OsPep4 peptide	Lifetein	N/A
PSK peptide	Lifetein	N/A
OsPSKR-8xHis-GFP protein	This paper	N/A
GST-OsPSKR-KD protein	This paper	N/A
GST-OsPSKR-ΔKD protein	This paper	N/A
GST-OsPSKR-CD protein	This paper	N/A
GST-OsPSKR-ΔCD protein	This paper	N/A
GST-AtEFR-CD	This paper	N/A
GST-AtEFR-ΔCD	This paper	N/A
Deposited data		
RNA-seq	This paper	GSE260646
Experimental models: Organisms/strains		
Rice: pskr KO1-3	This paper	N/A
Rice: 35S:amiRNA-OsPSKR	This paper	N/A
Rice: 35S:OsPSKR-GFP	This paper	N/A
Oligonucleotides		
Primers see Table S1	Sigma/Eurofins	N/A

(*Continued on next page*)

Continued

REAGENT or RESOURCE	SOURCE	IDENTIFIER
Recombinant DNA		
pRSF-duet-OsPSKR-8xHis-GFP	This paper	N/A
pGEX-6p1-OsPSKR-KD	This paper	N/A
pGEX-6p1-OsPSKR-ΔKD	This paper	N/A
pGEX-6p1-OsPSKR-CD	This paper	N/A
pGEX-6p1-OsPSKR-ΔCD	This paper	N/A
pGEX-6p1-AtEFR-CD	This paper	N/A
pGEX-6p1-AtEFR-ΔCD	This paper	N/A
pCAMBIA1380-35S:OsPSKR-GFP	This paper	N/A
pCAMBIA1380-35S:OsSERK1-HA	This paper	N/A
pCAMBIA1380-35S:OsSERK2-HA	This paper	N/A
pRGEB32-OsPSKR-gRNA(CRISPR)	This paper	N/A
pCAMBIA1380-35S:OsPSKR-amiRNA	This paper	N/A
pCAMBIA1380-35S:OsPEPR1-myc	This paper	N/A
pCAMBIA1380-35S:OsPEPR1-ΔKD-myc	This paper	N/A
Software and algorithms		
MO Affinity Analysis software	nanotemper	https://support.nanotempertech.com/hc/en-us/sections/17715198724753-Software#17715412421137
Trimmomatic	(Bolger et al., 2014)[83]	http://www.usadellab.org/cms/index.php?page=trimmomati
Hisat	(Kim et al., 2015)[84]	http://www.ccb.jhu.edu/software/hisat/
Cufflinks	(Trapnell et al., 2014)[85]	http://cufflinks.cbcb.umd.edu/

RESOURCE AVAILABILITY

Lead contact

Further information and requests for resources and reagents should be directed to and will be fulfilled by the lead contact, Padubidri V. Shivaprasad (shivaprasad@ncbs.res.in).

Materials availability

The materials generated in this study should be requested from the lead contact.

Data and code availability

- All data generated or analyzed during this study are included in this published article (and its supplemental information files).
- RNA-seq data is available under GEO accession number: GSE260646.
- Additional information required to repeat the analysis can be requested from the lead contact.

EXPERIMENTAL MODEL AND STUDY PARTICIPANT DETAILS

Plant materials and growth conditions

Oryza sativa indica PB1 variety was used in this study. Rice plants were grown in greenhouse at 28°C under natural day-night cycle. *N. benthamiana* plants used for infiltration experiments were grown in greenhouse conditions with natural day-night cycle.

Bacterial strains

Agrobacterium tumefaciens (LBA4404 with pSB1) harboring various indicated constructs was grown on YEB agar media at 28°C with antibiotics. The concentration of antibiotics for agar- 25 μg mL^{-1} rifampicin, 5 μg mL^{-1} tetracycline, 100 μg mL^{-1} kanamycin. The concentration of antibiotics for broth- 2.5 μg mL^{-1} tetracycline, 50 μg mL^{-1} kanamycin.

Agrobacterium tumefaciens (GV3101) harboring various indicated constructs was grown on YEB agar media at 28°C with antibiotics. The concentration of antibiotics for agar- 25 μg mL^{-1} rifampicin, 10 μg mL^{-1} gentamycin, 100 μg mL^{-1} kanamycin. The concentration of antibiotics for broth- 10 μg mL^{-1} gentamycin, 50 μg mL^{-1} kanamycin.

METHOD DETAILS

Plasmid construction and cloning

To generate CRISPR knock-out construct, guide RNA fragment was inserted into pRGEB32 vector[75] using BsaI sites. To generate amiRNA construct, amiRNA sequence was designed using WMD3[49,50] and inserted into pCAMBIA1380 (GenBank accession no. AF234301.1) vector under 35S promoter. To generate 35S:OsPSKR-eGFP (OE plants) plants, CDS of OsPSKR was inserted between SalI and NcoI sites, eGFP coding sequence was inserted between NcoI and SpeI sites of pCAMBIA1380 vector.

For all infiltration experiments derivatives of pCAMBIA1380 were used, 35S promoter sequence was amplified from pRT100 and inserted between EcoRI & BamHI sites. 35S:eGFP was generated by inserting eGFP sequence between BamHI & SalI sites. 35S:OsPSKR was generated as described above. 35S:OsSERK1-HA and 35S:OsSERK2-HA were generated by inserting OsSERK1-HA and OsSERK2-HA sequences between KpnI & SpeI sites in pCAMBIA1380. 35S:OsPEPR1-myc and 35S:OsPEPR1ΔKD-myc were generated by inserting respective coding sequences between SalI and SpeI sites in pCAMBIA1380. All vectors were mobilized into GV3101 strain of *Agrobacterium* and confirmed using colony PCR. Gene IDs of all the genes used are mentioned in Table S2.

Rice transformation

Rice transformation was carried out as described previously.[76,77] Rice seeds were dehusked and surface sterilized with 70% ethanol, 4% bleach and 0.1% mercuric chloride. Seeds were placed on callus induction media and kept in dark for 21 days. Calli were used for transformation with the desired constructs using LBA4404 (with pSB1) strain of *A. tumefaciens*. Calli were selected on hygromycin containing media in dark before transferring to regeneration media. Shoots derived from regeneration were transferred to ½ MS media for rooting before transferring to soil.

Transient expression through *Agrobacterium* infiltration

A. tumefaciens strain GV3101 harboring various constructs were grown in liquid YEB medium with appropriate antibiotics overnight in 28°C shaking incubator as described.[78] Cells were pelleted and resuspended in infiltration buffer containing 10 mM MES (pH 5.7), 10 mM MgCl2 and 100 μM acetosyringone. OD_{600} of the suspension was adjusted to 0.2. Three to four-week-old *N. benthamiana* plants were infiltrated using 1 mL needle-less syringes. Leaves were harvested 3 days post infiltration (dpi) for immunoblot and IP experiments. For super infiltration of PSK, 1 μM of peptide dissolved in water was used to infiltrate the leaves infiltrated with different *Agrobacterium* cultures containing different constructs after 3 dpi. Leaves were collected 20 min after infiltration unless otherwise mentioned.

Leaf wounding experiment

Six-weeks-old rice plants were used for wounding. Leaf blades were punched at the edges using a 3 mm punching equipment at a 2 cm interval without damaging midrib.[37] Leaves were collected at corresponding time points along with corresponding unwounded leaves and snap frozen before processing for experiments.

Peptide treatment

Six-week-old rice leaves were cut into leaf strips of 2 cm each. Leaf strips were maintained overnight in sterile water in six-well plates to wash away the residual wound signals as described previously.[79] Leaf strips were treated with 1 μM of peptides (custom made from Lifetein) and collected at the time points mentioned in the results section with corresponding mock treated samples.

RT-qPCR analyses

For qPCR analysis, extracted RNA was subjected to cDNA synthesis using Thermo RevertAid RT kit following manufacturer's protocol. The cDNA obtained was used for qPCR experiments using SYBR green master mix (Solis Biodyne- 5x HOT Firepol Evagreen qPCR master mix). *OsActin* gene primers were used as internal control. All the primers used are listed in Table S1. Gene IDs of all the genes used are mentioned in Table S2.

Transcriptome analysis

For RNA sequencing, six-week-old plants were used unless otherwise mentioned. Wounding was carried out as mentioned above and RNA was extracted from leaf samples using Trizol method of RNA extraction procedure. RNA was poly A enriched and Library preparation was carried out using NEBNext Ultra II Directional RNA Library Prep kit (E7765L) according to manufacturer's instructions. Sequencing was performed in a paired-end fashion on Illumina Hiseq2500 platform for all the sequencing and novaseq6000 for RNA-sequencing upon PSK treatment. RNA sequence analysis was carried out as described previously.[38] An average of 30 million paired-end reads were obtained from an Illumina Hi-seq platform. Adapter trimming was done with Trimmomatic.[80] Obtained reads were mapped to rice genome (IRGSP1.0) using HISAT2.[81] Cufflinks was used to obtain gene expression profiles and results are plotted using R.[82] A cut-off of $Log_2FC \geq 1.5$ was used for selecting upregulated genes and $Log_2FC \leq -1.5$ was used for selecting downregulated genes.

GO analysis

GO analysis was performed using ShinyGO v0.75 platform. RAPDB gene IDs were used with preference for biological processes with FDR cut-off of *p*-value:0.05.

Phylogenetic analysis

Extracellular amino acid sequences of the well-studied ligand binding receptors in *Arabidopsis* and rice were downloaded from TAIR (www.arabidopsis.org) and RAP-DB (https://rapdb.dna.affrc.go.jp/) respectively. Multiple sequence alignment of the receptors was performed using MUSCLE, with their extracellular region under default settings. A maximum likelihood phylogenetic tree was generated based on the alignment using MEGA v6.06[83] with the following parameters: Poisson correction and bootstrap values (1000 replicates). The tree was illustrated using iTOL v6 (https://itol.embl.de/).

Homology modeling and docking studies

Based on sequence similarity and phylogenetic relatedness, a 2.51 Å resolution crystal structure of the AtPSKR1 [PDB: 4Z63] was used as template to predict the 3D model of OsPSKR using MODELLER 9v22.[84] A set of 10 models were generated for the protein and the protein models with the least DOPE and molPDF scores were selected for final validation. Validation of model quality was carried out using Structure Analysis and Verification Server (SAVES), Protein Quality (ProQ) and Protein Structure Analysis (ProSA) servers. SAVES evaluates the quality of the protein model using various methods such as PROCHECK,[85] ERRAT[86] and VERIFY3D.[87] Structure visualization and analysis were performed using BIOVIA Discovery studio and ChimeraX.[88] Ligands retrieved from PubChem and chemspider database for the docking analysis in 3D SDF format were translated and stored in Mol2 format using Open Babel 2.2.3.[89] The energy minimized modeled OsPSKR structure was processed using the AutoDock tool. Molecular docking[90] was performed to identify the probable interacting residues between the modeled OsPSKR and the PSK ligand using AutoDock 4.2.1.[91]

Molecular dynamics (MD) simulation study

MD simulation studies were carried out as described[92] in order to determine the backbone configuration of receptor OsPSKR bound to PSK peptide ligand. To set up the simulation initially, the systems were built for OsPSKR receptor with and without the PSK ligand in the system builder. MD simulation study was carried out in Desmond vs. 2020–1. To set up the initial parameters of an orthorhombic box of 10 × 10 × 10 Å, Desmond system builder was used. The receptor OsPSKR and ligand-receptor complex were neutralized with NaCl by adding 0.15 M Na^+ ions. The prepared systems were relaxed using the Desmond default protocol of relaxation. An MDS run of 10 ns was set up at constant temperature and constant pressure (NPT) for the final production run. The NPT ensemble was set up using the Nosé-Hoover chain coupling scheme at a temperature of 300 K for final production and throughout the dynamics with relaxation time 1 ps. A RESPA integrator was used to calculate the bonding interactions for a time step of 2 fs. All other parameters were as described.[92] After the final production run, the simulation trajectories of OsPSKR receptor complexed with PSK were analyzed for the final outcome of RMSD, RMSF, and ligand RMSF, derived from the simulation studies.

Southern blotting

Southern blotting was performed as described previously.[93] Total DNA was extracted from rice using CTAB method.[94] Around 10 μg of DNA was used for digestion with the mentioned enzymes. After digestion the DNA was resolved on 0.8% gel in 1XTBE. The DNA was transferred to Zeta probe nylon membrane (Biorad) using capillary transfer method. Membrane was UV crosslinked post transfer. The probe (hygromycin resistance coding DNA) was PCR amplified from the corresponding plasmids used for transformation. The resultant probe was internally labeled with [α-P32] dCTP (BRIT India) using Rediprime labeling kit (GE healthcare) and used for hybridization of the membrane. Further membrane was subjected to washes followed by exposure to phosphor imaging screen and scanned using Typhoon scanner (GE healthcare).

sRNA northern protocol

Northern hybridization for detecting amiRNA was performed as described earlier.[95] Around 15 μg of RNA was resolved in a 15% acrylamide gel. Further, electroblotting was performed onto Hybond N+ membrane (GE healthcare). Hybridization was performed using T4 PNK end labeled oligonucleotides with [γ-P32] ATP in hybridization buffer (Ultrahyb buffer- Invitrogen).

Recombinant protein expression and purification

pGEX-6P-1 (GE healthcare) vector containing Glutathione S-Transferase (GST) tag at the N-terminal end was used for expression of cytosolic domains of OsPSKR and AtEFR. Catalytic residue and ATP binding mutants were generated by site directed mutagenesis (Primers used are listed in the Table S1). The residues mutated for OsPSKR were chosen based on the conservation of residues in other well studied kinases.[96] Catalytic mutants for AtEFR were generated based on previously published work.[47] Rosetta Gami DE3 (Novagen) cells were transformed with pGEX-6P-1 plasmids harboring cytosolic and mutant cytosolic domains of the above-mentioned proteins. Single colony was used to raise a primary culture of 15 mL in LB broth. The next day, 1% of the primary culture was used to raise a secondary culture of 2 L and culture was allowed to grow at 37°C until the OD_{600} of 0.5. Further, protein expression was induced by treatment of the culture with 0.3 mM of isopropyl β-D-1-thiogalactopyranoside (IPTG) and allowed to grow at 18°C overnight. Cells were pelleted at 5000 rpm for 1 h at 4°C and stored at −80°C until use. Further, cells were resuspended in lysis

buffer containing 50 mM Tris-HCl pH 8, 300 mM NaCl, 5% (v/v) glycerol, 5 mM β-mercaptoethanol (β-ME), 1 mM phenylmethylsulfonyl fluoride (PMSF), 0.01% IGEPAL, 0.5 mg/mL lysozyme and cOmplete protease inhibitor tablets with EDTA (Roche). Cells were lysed by sonication (65% amplitude, five cycles of 10 s pulse-on 15 s pulse-off for 2 min) and were subjected to centrifugation at 17,000 rpm at 4°C for 1 h. Supernatant fraction was filtered through 0.45 μm filters. Filtrate was passed through econo-columns (Bio-rad) containing protino glutathione agarose 4B beads (Cytiva) pre-equilibrated with buffer-A (50 mM Tris-HCl pH 8, 300 mM NaCl, 5% (v/v) glycerol, 5 mM β-ME). Flow-through was passed through the column again. Beads in the column were washed by buffer-A and then with buffer-B (50 mM Tris-HCl pH 8, 600 mM NaCl, 5% (v/v) glycerol, 5 mM β-ME) and then again with buffer-A. Protein bound to beads were eluted using 15 mM reduced glutathione prepared in buffer-A. Protein yield and purity was assessed by CBB-staining.

For purification of extracellular region of the protein, region coding from amino acids 44–698 without signal peptide and transmembrane region was tagged to 8x His and GFP tags adjacent to each other at the C-terminal. Codon plus cells of *E. coli* were transformed with the plasmids harboring above mentioned constructs. Pelleted cells were resuspended in lysis buffer containing 10 mM Bis-Tris pH 6, 300 mM NaCl, 5% (v/v) glycerol, 5 mM β-mercaptoethanol (β-ME), 1 mM phenylmethylsulfonyl fluoride (PMSF), 0.01% IGEPAL, 0.5 mg/mL lysozyme and cOmplete protease inhibitor tablets with EDTA (Roche). Cells were lysed by sonication (65% amplitude, five cycles of 10 s pulse-on 15 s pulse-off for 2 min) and were subjected to centrifugation at 17,000 rpm at 4°C for 1 h. Supernatant fraction was filtered through 0.45 μm filters. Filtrate was passed through econo-columns (Bio-rad) containing Ni-NTA beads (Qiagen) pre-equilibrated with buffer-A (10 mM Bis-Tris pH 6, 300 mM NaCl, 5% (v/v) glycerol, 5 mM β-ME, 5mM imidazole). Flow-through was passed through the column again. Beads in the column were washed by buffer-A and then with buffer-B (10 mM Bis-Tris pH 6, 600 mM NaCl, 5% (v/v) glycerol, 5 mM β-ME, 15mM imidazole) and then again with buffer-A. Protein bound to beads were eluted using 350 mM imidazole prepared in buffer-A. Protein yield and purity was assessed by CBB-staining. Further, protein was subjected to size exclusion chromatography and the appropriate fractions corresponding to required size were collected for experiments.

MPK activation assay

For MPK activation assay, wounded or PEP treated leaf samples were ground using liquid nitrogen. Five volumes of 2x Laemmli sample buffer was added to one volume of ground tissue and boiled at 95°C for 10 min as described.[47] Samples were centrifuged and resolved on a 10% SDS-PAGE gel. Proteins were transferred to supported nitrocellulose membrane and probed with p44/42 MAPK antibody from Cell Signaling Technology (CST) (9102) at 1:2000 dilution as described.[47] Bands were detected using Chemiluminescence detector (ImageQuant LAS 4000- GE healthcare).

MST assay

MST assay was performed to determine binding of PSK to OsPSKR. About 20 nM of purified OsPSKR-8xhis-GFP was mixed with 12 different dilutions of peptide (3:4), ranging from 2.2 mM to 0.096 mM in the buffer (Bis-Tris pH- 6.0, Nacl 150 mM and tween 20 0.1%). The reaction mixture was incubated for 5 min in ice and was subjected to high-speed centrifugation at 4°C for 10 min. After centrifugation, glass capillaries (Monolith, MO-K025) were loaded with the reaction mix and MST measurements were taken using Monolith NT.115 device (NanoTemper Technologies), using 60% LED power and 60% MST power. Analysis was performed using MO Affinity Analysis software and raw data was extracted to plot using GraphPad prism. Binding is represented as normalized fluorescence with respect to $\log_{10}$ values of ligand concentration.

In vitro protein kinase assay

To check the catalytic kinase activity of OsPSKR, *in vitro* kinase assay was performed as described with slight modification.[47] AtEFR cytosolic domain was used as positive control. About 100 ng for low concentration (+) and 1 μg of protein for higher concentration (++) were used. Proteins were incubated in 20 μL kinase buffer (50 mM Tris-HCl pH 7.4, 100 mM NaCl, 2.5 mM $MgCl_2$, 2.5 mM $MnCl_2$, 10 μM ATP, 5% (v/v) glycerol, 370 kBq γ^{32}P-ATP) at 30°C for 30 min. Reaction was stopped by adding 20 μL 2X Laemelli SDS loading buffer and boiling at 70°C for 5 min. Proteins were separated by SDS-PAGE and further exposed to phosphor-screen for 10 min. Exposed screen was scanned and imaged using molecular imager (GE).

Protein extraction, immunoblotting and IP

The samples were ground using mortar and pestle and around 200 mg tissue was taken for protein extraction as described previously.[97] Ground tissue was resuspended in 200 μL extraction buffer (100mM Tris-HCl pH 7.5, 1 mM EDTA, 150 mM NaCl, 1% Triton X-100, 0.1% SDS, 10 mM dithiothreitol (DTT) and 1x protease inhibitor cocktail). Equal amount of 6x SDS-PAGE loading buffer was added and the samples were boiled at 95°C for 10 min, and then the samples were centrifuged at 13000 rpm for 10 min. Supernatant was collected in a fresh tubes and samples were resolved on 8% SDS-PAGE gels. Proteins were transferred to nitrocellulose membrane. Membrane was blocked with 5% milk and probed with primary antibodies anti-GFP (Sigma) and anti-HA (CST). Further, the membranes were probed with anti-rabbit secondary antibody and imaged using image quant. Same procedure was followed for protein extraction from rice leaves except that 1% (w/v) PVP was added to the extraction buffer.

For IP, leaves of infiltrated *N. benthamiana* plants were harvested at 3 dpi. For rice, six-week-old plants were used. IP was performed as described previously.[98] Around 2.5 gm of ground tissue was resuspended in 3 mL of extraction buffer (50 mM Tris-HCl pH 7.5, 150 mM NaCl, 2 mM EDTA, 10% glycerol, 2 mM DTT, 2 mM Phenylmethanesulfonyl Fluoride (PMSF), 1% Triton X-, 1x

protease inhibitor cocktail) and homogenised for 15 min at 4°C. Further, additional 9 mL of extraction buffer without Triton X- was added and homogenised for 30 min at 4°C. Samples were centrifuged at 5000 rpm at 4°C and supernatant was passed through 0.45 μM cell strainers. Then, 30 μL of GFP-trap (Chromotek) beads were added to each sample and binding was allowed for 3 h at 4°C with slow rotation on roto-spin. After binding, beads were collected using magnetic stand and subjected to three washes with wash buffer (50 mM Tris-HCl pH 7.5, 150 mM NaCl, 1 mM PMSF). Proteins were eluted from the beads by boiling with 50 μL of 2x SDS buffer at 80°C. Proteins were resolved on 8% SDS-PAGE gels and detected using WB.

SEM imaging and micro-computed tomography (micro CT)

SEM imaging was carried out as described previously.[99] Rice spikelets were collected prior to flowering and were fixed in 16% formaldehyde, 25% glutaraldehyde and 0.2 M cacodylate buffer for 12–16 h. Further, samples were washed with double distilled water and subjected to series of dehydration using series of 25–100% ethanol. Samples were then dried using Leica EM CPD300, gold coated, and imaged using a Carl Zeiss scanning electron microscope at an accelerating voltage of 2kV.

Pollen staining

Pollen grains viability test was performed using I_2-KI staining solution containing 0.2% (w/v) I_2 and 2% (w/v) KI as described.[99] Anthers from (n = 6) spikelets of mature two individual panicles just one day before the fertilization were collected in 100 μL of I_2-KI solution. Pollen grains were released in the solution by mechanical shearing using micro tips. After 10 min viable pollen grains in 20 μL solution were counted under bright-field microscope (Olympus BX43). Round and dark blue were considered as viable pollen grains, while light blue or distorted shape pollens were considered as nonviable.

DAB staining

DAB staining procedure was performed as described previously.[100] Leaves were immersed in DAB staining solution (dissolved 1 mg/mL of DAB by reducing the pH to 0.3 using 0.2 M HCl, further added 0.05% (v/v) tween 20 and 200 mM Na_2HPO_4 to obtain 10 mM Na_2HPO_4 DAB staining solution) overnight on a rotor. Samples were bleached using bleaching solution (ethanol: acetic acid: glycerol – 3:1:1) and washed thrice for 10 min each with boiling.

Trypan blue staining

Trypan blue staining solution (for 40 mL–10 mL of lactic acid (85% w/w), 10 mL of phenol (TE buffer equilibrated, pH 7.5–8.0), 10 mL of glycerol, 10 mL of distilled water, 1 mg/mL of trypan blue) was prepared and leaf samples were stained for 1 has described.[65] Samples were destained by giving repeated washes with 100% ethanol.

Callose staining and imaging

About 0.01% of aniline blue in KPO_4 buffer pH-7.5 was used for staining leaf samples. Staining was performed at room temperature overnight. Stained samples were imaged using confocal microscopy (Carl Zeiss LSM980). Excitation wavelength of 420–480 nm and emission wavelength of 495–550 was used as described previously.[101]

QUANTIFICATION AND STATISTICAL ANALYSIS

For all the RT-qPCR experiments, pairwise Student's t-test was used to compare between test and control expression of the genes indicated in the paper. The data is represented as relative expression and the error bars are for standard error calculated using standard deviation. The number of replicates used for qPCR was 3 and it is indicated in all the corresponding figure legends. Student's t-test was performed in excel. The gene-overlap significance was tested by performing Fisher's exact test in R using hypergeometric distribution of the overlapping genes in comparison to total number of genes in rice. The number of genes and the obtained p-value is mentioned in the corresponding figures. For the boxplots, the gene expression is represented as ASINH converted values of FPKM. The p-values were calculated using Wilcoxon test and are mentioned in the corresponding figures. The test was performed in R.